



Title	LC/MS/MS-based metabolic profiling for the improvement of <i>Synechococcus elongatus</i> 1-butanol-producing strains
Author(s)	Fathima, Artnice Mega
Citation	大阪大学, 2019, 博士論文
Version Type	VoR
URL	https://doi.org/10.18910/73547
rights	
Note	

The University of Osaka Institutional Knowledge Archive : OUKA

<https://ir.library.osaka-u.ac.jp/>

The University of Osaka

DOCTORAL DISSERTATION

**LC/MS/MS-based metabolic profiling for the improvement
of *Synechococcus elongatus* 1-butanol-producing strains**

Artnice Mega Fathima

July, 2019

Department of Biotechnology,
Graduate School of Engineering,
Osaka University

This thesis is dedicated to my beloved parents who have always been a source of encouragement to undertake my higher education and to face the eventualities of life with patient, enthusiasm, and fear of Allah

“But perhaps you hate a thing and it is good for you; and perhaps you love a thing and it is bad for you. And Allah Knows, while you know not.”

2:216

Contents

Contents.....	1
List of abbreviations.....	4
Chapter 1.....	5
General Introduction.....	5
1.1 1-Butanol as commodity chemical and advanced biofuel	5
1.2 Microbial-based 1-butanol production.....	7
1.3 <i>Synechococcus elongatus</i> 1-butanol-producing strains	11
1.4 Metabolomics approach for strain improvement.....	14
1.5 LC/MS/MS widely targeted metabolic profiling.....	17
1.6 Objective of this study.....	19
1.7 Research outline	19
Chapter 2.....	22
Improvement of butanoyl-CoA to butanal reaction in 1-butanol biosynthesis pathway results in higher production of 1-butanol.....	22
2.1 Introduction.....	22
2.2 Materials and methods	25
2.2.1 Cyanobacterial strains and plasmids	25

2.2.2 Culture medium and growth conditions	26
2.2.3 Sampling and extraction	27
2.2.4 Ion-pair reversed-phase LC/QqQ-MS analysis	28
2.2.5 1-Butanol analysis	29
2.2.6 Data analysis.....	30
2.2.7 PduP enzyme assay.....	30
2.3 Results and discussion	32
2.3.1 Comparative metabolite analysis of EL22 and BUOHSE identified a possible target for strain improvement in 1-butanol biosynthesis	32
2.3.2 Enhancing 1-butanol titers by improving PduP enzyme activity	39
Chapter 3	41
Optimization of acetyl-CoA to malonyl-CoA reaction enables high titer and productivity of 1- butanol	41
3.1 Introduction	41
3.2 Materials and methods	43
3.2.1 Cyanobacterial strains and plasmids	43
3.2.2 Culture medium and growth conditions	44
3.2.3 Sampling and extraction	44

3.2.3 Absolute quantification of CoA-related metabolites	45
3.2.4 Ion-pair Reversed-Phase LC/QqQ-MS analysis.....	46
3.2.5 1-Butanol analysis	46
3.2.6 Data analysis.....	46
3.2.7 RNA extraction and <i>Reverse Transcription</i> Polymerase Chain Reaction (RT-PCR)	46
3.3 Results and discussion	47
3.3.1 Characterization of DC7 strain by widely targeted metabolic profiling	47
3.3.2 Optimization of ACCase enzyme to divert enhanced level of acetyl-CoA towards 1- butanol formation.....	52
3.3.2 Characterization of DC11 strain by LC/MS/MS system.....	55
Chapter 4	57
Conclusions and future perspectives	57
Acknowledgement	63
References	65
List of publication	74
Appendix	76

List of abbreviations

nphT7: acetoacetyl-CoA synthase

bldh: CoA-acylating butanal dehydrogenase

yqhD: NADPH-dependent alcohol dehydrogenase

phaJ: (*R*)-specific crotonase

phaB: acetoacetyl-CoA reductase

pduP: CoA-acylating propionaldehyde dehydrogenase

ACCase: acetyl-CoA carboxylase

Kan^R: Kanamycin Resistance

Gen^R: Gentamycin Resistance

IP-RP-LC/QqQ-MS: Ion-Pair Reversed-Phase Liquid Chromatography Triple Quadrupole

Mass Spectrometer

PCA: Principal Component Analysis

RBS: Ribosome Binding Site

IPTG: Isopropyl β-D-1-thiogalactopyranoside

BG-11: Blue-Green 11

RT-PCR: *Reverse Transcription* Polymerase Chain Reaction

Chapter 1

General Introduction

1.1 1-Butanol as commodity chemical and advanced biofuel

1-Butanol, an aliphatic saturated C₄ alcohol with molecular formula (C₄H₁₀O) [1], is considered as an important commodity chemical and an advanced biofuel [2]. It can be used directly as solvents or converted into its derivatives for producing a variety of chemicals and materials, including solvents, fuels, polymers, pharmaceuticals, perfumes, and food [3]. Besides its chemical applications, this alcohol has also received significant attention as potential fuel to displace gasoline. The advantages of 1-butanol over other biofuel targets are its hydrophobicity and high energy density. In addition, it is suitable for current infrastructure and also offers safety advantages as a transportation fuel since the vapor pressure of 1-butanol is much lower than ethanol under normal atmospheric condition (see Table 1.1-1). The physicochemical properties of 1-butanol have similar features to those of gasoline [2].

Table 1.1-1. Comparison of chemical and physical properties of gasoline and diesel to advanced biofuels: ethanol and 1-butanol [2], [4].

Fuel	Energy Density of vaporization (MJ/L)	Heat (MJ/kg)	Octane Number	Solubility in water (%)	Air-to-Fuel Ratio
<i>Gasoline</i>	32	0.36	81-89	immiscible	14.6
<i>Diesel</i>	35.5	nd-no data	nd-no data	immiscible	14.7
<i>Ethanol</i>	19.6	0.92	96	100	8.94
<i>1-Butanol</i>	29.2	0.43	78	7	11.12

Currently 1-butanol is mainly synthesized through chemical processes, such as crotonaldehyde hydrogenation or oxo synthesis, at a cost of 7.0–8.4 billion dollars per year [2]. However, these methods are no longer being considered for production of alternative fuel constituent due to economic reasons. Thus, fermentation-based production —the so-called acetone-butanol-ethanol (ABE) fermentation, using various bioresources and the Gram-positive bacteria, *Clostridium* sp., was considered as a promising alternative. However, low-yield, low 1-butanol tolerance, and the high cost of the fermentation substrates, as well as downstream processing have been known to be the main hurdles for improving ABE fermentation production system [2].

1.2 Microbial-based 1-butanol production

Butanol production through fermentation process was first introduced in 1862 (Pasteur, 1862). At this time, Louis Pasteur reported this alcohol to be a fermentation product of *Vibrio butyrique*—though it was a result of mixed culture, some *Clostridium* strains may have been present in the culture [5]. Due to a shortage of natural rubber in the beginning of 20th century, demand for synthetic rubber production increased. This need then stimulated commercial interest of microbial fermentation for producing bulk chemicals (Fig. 1.2-1) [6], [7].

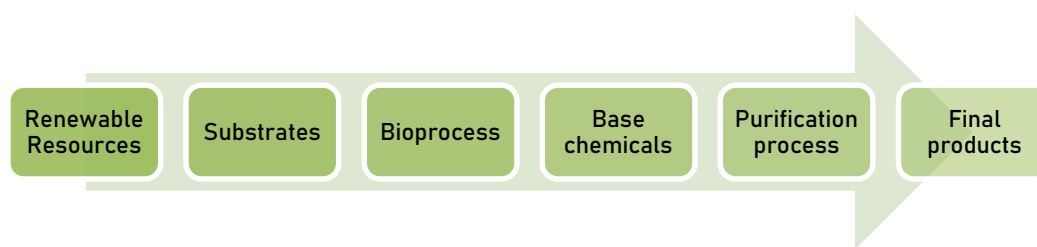


Figure 1.2-1. Schematic of microbial fermentation-based production from renewable resources into final products.

Microbial-based production was investigated further by a number of researchers [8] and among those working, Chaim Weizmann succeeded in isolating microorganisms with the ability to produce acetone and butanol. The demand of acetone production kept increasing which led to the development of ABE fermentation on industrial scale, utilizing *C. acetobutylicum*. This large scale production resulted in up to 3000 tons of acetone and 6000 tons of butanol [7], [8]. Approximately 66% and 10% of the world's supply of butanol and acetone, respectively, was

achieved by ABE fermentation. However, in mid-20th century low-yield and difficulties for maintaining anaerobic condition for ABE fermentation made it unable to economically compete with petrochemical technology [5]. Therefore, this process was largely forgotten in the past several years. Nowadays, due to the high concern regarding energy sustainability, environmental pollution, the usage of toxic compounds and the effort to decrease carbon footprint, microbial-based butanol production is regaining its popularity. Recent studies have been focusing on optimizing fermentation processes and/ or strain development using metabolic engineering tactic, in order to meet industrial competitiveness [7].

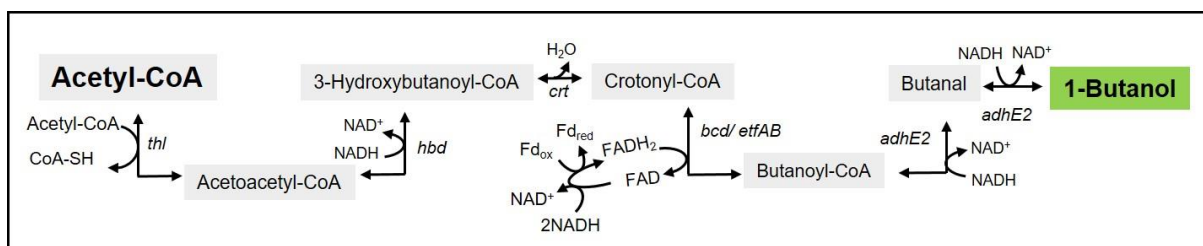


Figure 1.2-2. Schematic representation of CoA-dependent pathway in *Clostridia* species.

Selected species of *Clostridia* natively produce 1-butanol via a natural metabolic CoA-dependent pathway [5]. This native clostridium pathway proceeds by condensation of two acetyl-CoA and follows a series of reduction steps using NADH, finally resulting in dehydration to form 1-butanol (Fig. 1.2-2) [9], [10]. The advancement of molecular genetic technology has been allowing some researchers to engineer metabolic pathways of various microorganisms,

enabling integration of CoA-dependent pathways into other standard microbial production hosts [11].

Theoretically, this metabolic engineering strategy can be realized in any production host, provided that the genetic toolbox of that particular organism is well studied. However, some genetic traits are more difficult to be engineered than others practically, thus making the selection of parental strains to be considered as a crucial step for designing the experiment [11]. In particular, the availability of synthetic biological tools, the tolerance level towards the target products, and the carbon sources that will be utilized, are important factors to be considered [6], [12].

The successfulness of metabolic pathway engineering is greatly affected by the availability of information on genotypic characteristics and genetic tools for gene transfer purposes. The uniformity of biological traits, such as promoters, ribosome binding sites and other regulatory elements, allows researchers to rebuild the entire genome of particular microorganism [12]. Furthermore, metabolic engineering also enables the researcher to design the microbial host to secrete its synthesized product, thereby avoiding product extraction step [13]. *Escherichia coli* and *Saccharomyces cerevisiae* are two most widely researched model organisms and are hence well-characterized microbes. Therefore, these two microbial hosts are commonly used as cell factories [12]. Among photosynthetic organisms, cyanobacterium *Synechococcus elongatus*

PCC 7942 has been used as a model organism. Although the current state of knowledge regarding genome engineering in cyanobacteria moves relatively slower compared to other model organisms, the toolbox itself has been improved significantly over the last few years [12]. In addition to the genetic knowledge, cell tolerance towards the product of interest is important and must be considered. The utilization of native producer is indeed more beneficial in term of tolerance compared to non-native producer. However, in case the synthesis pathway is tightly regulated by certain condition, such as for obligate anaerobes, the production efficiency may be hampered. Thus, choosing a host microorganism that can be grow easily in various conditions may help increase production efficiency [12], [14].

In regards to substrate selection, edible feedstock has been used as substrate which includes starch-based or sugars-based substrates for the 1st generation of biofuels. However, several problems have emerged with the use of edible feedstock for biofuel production. Use of edible feedstocks could result in rising food costs, land competition and ineffective production processes [14]. To overcome this problem, the range of raw materials utilized has been expanded. Ligno-cellulosic-based production was then known as 2nd generation biofuels. However, production of 2nd generation biofuels still remains challenging. Despite the fact that the ligno-cellulosic feedstocks are cheaper, additional cost for pretreatment process is necessary to make the substrate ready to be fermented by the microbial producer. Therefore, high cost

production still remains the major constraint for industrial application [15]. Generally, the definition of biofuels is not only limited as fuels that are produced from biomass by either biological or non-biological processes, but also includes fuels that are generated from other renewable resources, such as carbon dioxide (CO₂), through biological processes [14]. In relation to that, direct conversion of CO₂ to produce valuable products using photosynthetic organisms, like cyanobacteria, has garnered significant interest for its prospective role in attaining a carbon neutral society. Furthermore, the key advantage of using cyanobacteria as a platform strain over other model organisms is the ability of this microorganism to utilize CO₂ as carbon source and sunlight as energy source, hence making the addition of substrate unnecessary [16]. This strategy is believed to be able to minimize the land competition and feedstock cost. Overall, cyanobacterial-based 1-butanol production can be an attractive candidate for production of 1-butanol in a sustainable manner.

1.3 *Synechococcus elongatus* 1-butanol-producing strains

In relation to the aforementioned background, a cyanobacterial strain capable of producing 1-butanol was engineered by introducing a modified *Clostridial* CoA-dependent pathway (Fig. 1.3-1A) [17]–[19]. Cyanobacterium *Synechococcus elongatus* PCC7942 was selected as parent strain owing to its fast growth and genetic tractability compared to other strains [20]. There are

several strains which have been successfully engineered to produce 1-butanol such as EL22 and BUOHSE strains. Several modifications have been done in the CoA-dependent pathway by means of metabolic engineering tactic to improve 1-butanol production in both engineered-strains. Initially, ATP-driven malonyl-CoA-mediated reaction was utilized in EL22 strain to drive carbon flux into the formation of acetoacetyl-CoA (Fig. 1.3-1B). This modification was apparently able to force the thermodynamically unfavorable condensation reaction of acetyl-CoA forward [18]. Furthermore, the NADH-dependent enzymes (Hbd, AdhE2) in native CoA-dependent pathway (Fig. 1.3-1B) has been replaced with NADPH-dependent enzymes (PhaB, Bldh, and YqhD) (Fig. 1.3-1B) allowing 1-butanol production in *Synechococcus elongatus* EL22 to reach 29.9 mg/L.

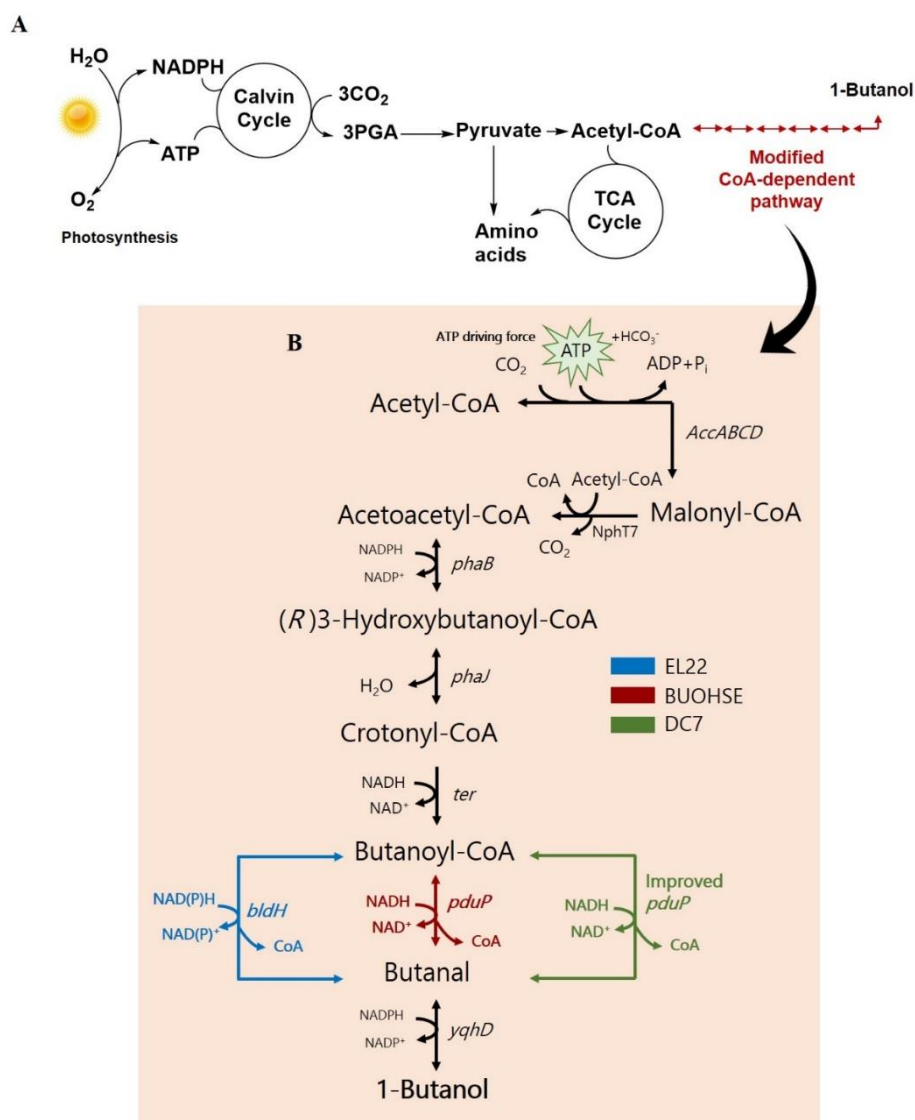


Figure 1.3-1. (A) 1-Butanol pathway in *S. elongatus* strain. (B) A modified CoA-dependent pathway in the BUOHSE strain.

However, in EL22 strain, the conversion of butanoyl-CoA to butanal was engineered using an oxygen-sensitive enzyme, named CoA-acylating butanal dehydrogenase (Bldh). This became a serious problem for 1-butanol production owing to the photosynthesis process that evolves oxygen in cyanobacteria. Since oxygen sensitivity of Bldh hindered 1-butanol production, it

was replaced with an oxygen-tolerant enzyme (PduP) resulting in strainthe BUOHSE, which displayed a significant increase in 1-butanol production, 317 mg/L [18], [19]. Regardless, the final 1-butanol titer of BUOHSE was still low compared to other microbial hosts. Therefore, the main focus of this thesis is on improving both titer and productivity of *S. elongatus* 1-butanol producing strain.

1.4 Metabolomics approach for strain improvement

Some vigorous efforts have been made to boost microbial-based 1-butanol production in microorganisms through several approaches, including utilization of various carbon sources, elimination of undesired product, deletion of competing pathways, improvement of cell density, and improvement of tolerance towards the product [9], [14], [16], [21]–[29].

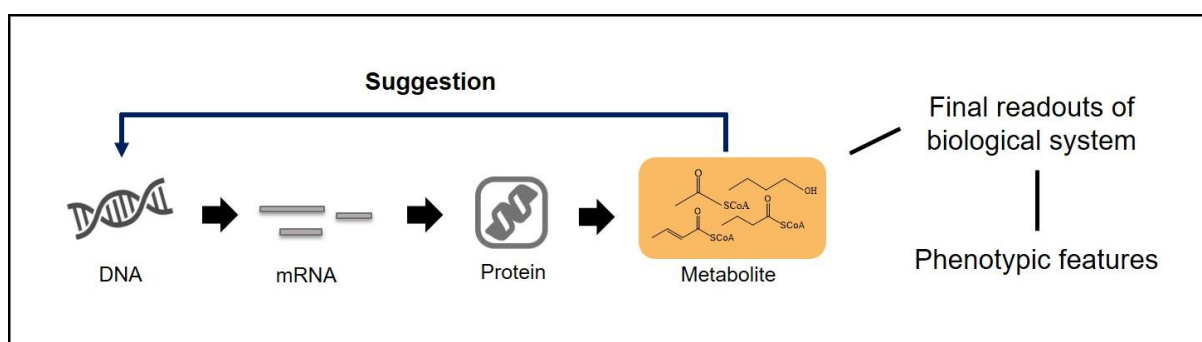


Figure 1.4-1. Schematic of metabolomics-assisted strain engineering

The most common approach for selection of target gene to improve the production is rational selection, whereby the gene targets are chosen based on genetic knowledge. However due to competition among researchers for development of an appropriate host for industrial

scale production, rational selection approach is often ineffective, resulting in unexpected cellular behaviors [29]. On the other hand, metabolomics, a comprehensive study of metabolites, is able to demonstrate the downstream effects of gene and protein regulation, representing closest correlation with phenotypic features [30], [31] (Fig 1.4-1). In combination with multivariate data analysis (MVDA) tools like principal component analysis, important metabolites in a biological system can be selected and ranked unbiasedly. Moreover, combined metabolomics and MVDA approach is also beneficial for resolving common problems in microbial related work, such as characterization of engineered strains, identification of putative bottleneck reactions, investigation of any possible competing pathways, optimization of growth medium, and exploration of potential products of the strains [32]. Therefore, a deeper understanding of the metabolic state of 1-butanol-producing strains offers an effective way to facilitate strain improvement.

The main challenge in microbial metabolomics is to assure that the obtained samples accurately snapshot the real cellular metabolic condition. Thus, the target of metabolites analyzed and the procedure of sample collection must be considered carefully. First, it is essential to determine the target metabolites to be compared within different samples. When studying bioproduct improvement, widely targeted metabolic profiling is particularly preferred over non-targeted profiling to allow a statistically reliable interpretation of the data [32]. Thus,

in this work, widely targeted metabolic profiling using ion-pair reversed phase liquid chromatography triple quadrupole mass spectrometer (IP-RP-LC/QqQ-MS) system [21], [33], [34] was employed to investigate metabolic states of *S. elongatus* 1-butanol producing strains.

Another aspect of microbial metabolomics that requires consideration is the procedure to generate and collect the microbial samples. During cultivation of microorganisms for instance, the medium and sample preparation used may result in variation of the samples [31], [32]. Therefore, it is important to ascertain that cells are able to grow in reproducible manner. Moreover, in order to acquire metabolome snapshots which represents the metabolic state of the cells accurately, rapid sampling and quenching techniques are required. These two steps need to be considered carefully to avoid metabolites loss or any introduction or conversion of metabolites in the samples during the harvesting process. In addition, sample extraction is also one of the steps that is highly prone to introduce variation and errors in the sample data. This step has to be optimized and minimized to restrain changes in metabolite composition due to enzymatic activities that are still present in the samples. In this thesis, samples collection and preparation for *Synechococcus elongatus* PCC 7942 has been optimized for LC/MS/MS analysis and details are described in the materials and method section.

1.5 LC/MS/MS widely targeted metabolic profiling

As the previous study was only limited to the CoA-dependent pathway, there is a possibility that other targets that need to be improved are present within the 1-butanol producing strain. In widely targeted analysis, the target metabolites are selected by employing QqQ/MS in Multiple Reaction Monitoring (MRM) mode. The MRM mode works in two stages of selection processes. In the first selection, a precursor ion is preselected in Q1 and then its fragments are selected in Q3, while in Q2 fragmentation of the precursor ion occurs [35]. This form of analysis is suitable for metabolic profiling due to its high sensitivity and wide dynamic range [33]. The use of ion-pair reversed phase liquid chromatography triple quadrupole mass spectrometer (IP-RP-LC/QqQ-MS) has been shown to have a wide coverage of metabolites in separating and analyzing polar metabolites from central metabolism [36]. For the analysis of cyanobacteria samples, IP-RP-LC/QqQ-MS with C18 column was optimized to cover as many metabolites as possible, especially the ones related to or involved in the central metabolism. During the course of this study, 74 metabolites including sugar phosphates, amino acids, organic acids, and cofactors in central metabolism were selected as target metabolites.

Advancement in metabolomics allow not only the identification of what metabolites are present in the cell, but also the quantification of each existing metabolite [31]. Metabolite

quantification is not always necessarily on an absolute scale. Relative scale can also be performed by comparing the acquired peak areas of the same metabolites in different samples. Moreover, to allow comparison of relative concentrations of metabolites analyzed, internal standard addition prior to the extraction and analysis steps is required for sample normalization [32]. Next, after data preprocessing, the obtained relative concentration of metabolites can be subjected to MVDA.

The most commonly used tools in MVDA is principle component analysis (PCA). PCA transforms strongly correlated variables into a new variable, named principal component (PC) [30], [32]. From the PCA analysis, a score plot and loading plot will be generated. The score plot is able to explain whether samples are similar or dissimilar by arranging samples in clusters. When the sample clusters do not overlap with each other, it can be assumed that there may be significant information in the metabolome which contributes to that clustering result. The important metabolites which contribute most to the clustering result can be reflected from its loading plot. MVDA tools are mainly applied as predictive tools to generate hypothesis from the metabolome data, as well as to extract the hidden information in the data sets [32]. Specifically, the important metabolites that explain the differences between the samples, and the cause of co-vary in all the data sets can be realized [32]. This kind of MVDA information is useful for strain improvement.

1.6 Objective of this study

As described above, the current state of strain improvement for *Synechococcus elongatus* 1-butanol producing strain lags far behind of other microbial hosts. The latest highest 1-butanol titer was reported in 2013 by Liao group. Thus, in order to better facilitate strain improvement, metabolomics approach was applied in this study. The overall objective of this study is, to improve 1-butanol titer and productivity in *Synechococcus elongatus* 1-butanol producing strain by identifying possible target for strain improvement in the 1-butanol biosynthesis pathway, meanwhile demonstrating the power of metabolomics in discovering and solving pathway engineering problems. The first finding of a possible target for strain improvement in the CoA dependent pathway and its genetic modification is described in the Chapter 2. Moreover, the new strategy to solve the second target, and improvement in 1-butanol productivity step is described in Chapter 3.

1.7 Research outline

This thesis gives an overview of the utility of metabolomics in metabolic engineering. Specifically, comparative metabolome analysis of *S. elongatus* 1-butanol producing strains was able to identify target that needed to be improved in cyanobacterial 1-butanol biosynthesis pathway (CoA-dependent pathway). Furthermore, with metabolic engineering techniques,

modifications in the CoA-dependent pathway were carried out effectively. Subsequently, the highest titer and productivity to be reported was achieved in engineered *S. elongatus* PCC7942 based on the obtained insight from metabolomics.

In **Chapter 2**, comparative metabolome analysis of BUOHSE with the low producing strain (EL22) was carried out to identify targets within the 1-butanol biosynthetic pathway that required further improvement. Briefly, the data confirmed that the reduction reaction from butanoyl-CoA to butanal, which is catalyzed by PduP enzyme, was the target reaction that needed to be improved in the CoA-dependent 1-butanol pathway. In addition, high accumulation of acetyl-CoA in CoA-dependent pathway was also observed from this comparison. Subsequently, genetic modification based on the aforementioned finding was performed via the replacement of the original ribosome binding site (RBS) upstream of *pduP* in BUOHSE. The new strain, named DC7, outperformed the 1-butanol titer of BUOHSE by 33% and exhibited a decreased level of butanoyl-CoA. This indicated that the butanoyl-CoA to butanal reaction was successfully improved which led to the increased titer of 1-butanol.

In **Chapter 3**, in order to understand the overall effect of PduP optimization, metabolome comparison of BUOHSE and DC7 was done which showed acetyl-CoA was highly accumulated in DC7 strain. Accordingly, to utilize this enhanced level of acetyl-CoA for 1-butanol formation in DC7, acetyl-CoA carboxylase (ACCase) was selected as the next target

for strain improvement. Genetic modification involved two main strategies: 1) disruption of *aldA* gene, encoding for alcohol dehydrogenase, to eliminate any unwanted consumption of acetyl-CoA and 2) introduction of *accase* gene from *Yarrowia lipolytica* into the disruption site. This engineering strategy resulted in a strain, named DC11, which achieved a maximum 1-butanol titer of 117 mg/L per day between days 4 and 5, outperforming the first reported high 1-butanol producing strain BUOHSE by 57% (74.5 mg/L per day).

In **Chapter 4**, the summary of important conclusions obtained from this study and the future perspectives are described.

Chapter 2

Improvement of butanoyl-CoA to butanal reaction in 1-butanol biosynthesis pathway results in higher production of 1-butanol

2.1 Introduction

1-Butanol is considered an important commodity chemical and advanced biofuel [3]. Thus, the introduction of a CoA-dependent pathway to produce 1-butanol in various host organisms such as *Escherichia coli* [9], [21], *Saccharomyces cerevisiae* [37], *Pseudomonas putida*, *Lactobacillus brevis*, *Bacillus subtilis* [24], [38] and Cyanobacterium *Synechococcus elongatus* [17] has become a common strategy for microbial production. In relation to this, to allow 1-butanol production in a sustainable manner, photosynthetic organisms such as cyanobacteria have recently become attractive model microorganisms because of their ability to convert carbon dioxide to valuable products [39]–[41]. Thus, cyanobacterial strain capable of producing 1-butanol was engineered by introducing a modified *Clostridial* CoA-dependent pathway [18], [19]. Initially, *Synechococcus elongatus* strain EL22 was engineered using an oxygen-sensitive enzyme, CoA-acylating butanal dehydrogenase (Bldh), for conversion of butanoyl-CoA to butanal and was able to produce a low titer of 29.9 mg/L of 1-butanol [18].

Since oxygen sensitivity of Bldh hindered 1-butanol production, it was replaced with an oxygen-tolerant enzyme (PduP) in the BUOHSE strain, which resulted in a significant increase in 1-butanol production [19].

In recent years, metabolomics-based approaches for strain improvement are widely being employed. This rapidly growing field, focusing on the whole metabolite profile of a biological system, provides valuable information that can be applied in numerous ways [21], [29], [33], [34], [42]. By means of rapid detection of relevant metabolic perturbations, metabolomics can identify specific targets for strain improvement that may include identification of rate limiting steps in a production pathway, metabolite or product toxicity, cofactor imbalances, or depletion of metabolites consumed by alternative pathways [21]. Therefore, a deeper understanding of the metabolic state of 1-butanol-producing strains can facilitate strain improvement by further strain modifications.

Previously, a targeted metabolomics analysis focusing on the CoA-dependent pathway in 1-butanol producing *S. elongatus* strain was performed by our previous research group [42]. In this published work, strains that differ in enzymes that convert butanoyl-CoA to butanal were compared. The introduction of an oxygen tolerant (PduP) enzyme to replace the oxygen sensitive (Bldh) enzyme was intended to increase the activity of this reaction in strain BUOHSE from base strain EL22 (Fig 1.3-1B). As a result, a major increase in 1-butanol titer was observed

in BUOHSE compared to EL22 (Fig 2.3-1A). Consequently, decrease in the amount of butanoyl-CoA in BUOHSE relative to EL22 due to a more effective conversion of butanoyl-CoA to butanal by the PduP enzyme was expected to be observed. Surprisingly, the metabolome data indicated that the amount of butanoyl-CoA was comparable to that of EL22 (Fig. 2.3-1C). Further analysis using kinetic profiling showed that the release of CoA resulting from the introduction of *pduP* in BUOHSE enabled free CoA regeneration that in turn led to the increased rate of acetyl-CoA synthesis. Here, the release of free CoA facilitated the reaction from pyruvate to acetyl-CoA, which was then used in the butanol pathway [42]. These facts strongly indicated that the reductive reaction of butanoyl-CoA to butanal should be modified further to improve 1-butanol productivity in the engineered cyanobacterial strain. Therefore, in this study, further optimization of the PduP enzyme to facilitate a more effective conversion from butanoyl CoA to butanal was carried out. In addition, since the previous analysis was only limited to the CoA-dependent pathway, there is a possibility that other possible targets are still present within the 1-butanol producing strain. Thus, widely targeted metabolic profiling was used to broaden the coverage of the metabolites analyzed, allowing for the identification of new possible targets in the 1-butanol biosynthesis pathway to ultimately improve both titer and productivity.

2.2 Materials and methods

2.2.1 Cyanobacterial strains and plasmids

Synechococcus elongatus strains and plasmids used in this study are listed in Table 2.2-1.

Cyanobacterial transformation and plasmid construction are described in our previous work [18], [19]. Salis calculator [43], [44] is used as a tool to generate different RBS sequences and replace the original RBS for *pduP* on the plasmid pSR3. Strain EL9 [17] was transformed with plasmid pDC304 containing a synthetic RBS sequence TCACAAAATACTTACCAACAAAGGAGGATCCC in front of *pduP*, resulting in a new strain DC7. (Strain constructions were done in UCLA by collaborator, Derrick Chuang)

Table 2.2-1. Strains and plasmids used in this study^a

Cyanobacteria strain	Genotype	Reference
EL22	P _{Trc} :: His-tagged <i>T. denticola ter</i> integrated at NSI and PL _{lacO1} :: <i>nphT7</i> , <i>bldh</i> , <i>yqhD</i> , <i>phaJ</i> , <i>phaB</i> integrated at NSII in PCC 7942 genome	[18]
BUOHSE	P _{Trc} :: His-tagged <i>T. denticola ter</i> integrated at NSI and PL _{lacO1} :: <i>nphT7</i> , <i>pduP_S. enterica</i> , <i>yqhD</i> , <i>phaJ</i> , <i>phaB</i> integrated at NSII	[19]

BUOHSE without pduP	P _{Trc} :: His-tagged <i>T. denticola ter</i> integrated at NSI and PL _{lacO1} :: <i>nphT7</i> , <i>phaJ</i> , <i>phaB</i> integrated at NSII	[42]
DC7	P _{Trc} :: His-tagged <i>T. denticola ter</i> integrated at NSI and PL _{lacO1} :: <i>nphT7</i> , <i>PduP_S. enterica</i> , <i>yqhD</i> , <i>phaJ</i> , <i>phaB</i> integrated at NSII, synthetic RBS TIR: 522266.72 in front of <i>pduP</i>	This work [45]
Plasmid	Genotype characteristic	Reference
pSR3	Kan ^R ; NSII targeting; PL _{lacO1} :: <i>nphT7</i> , <i>yqhD</i> , <i>pduP</i> , <i>phaJ</i> , <i>phaB</i>	[19]
pEL256	Kan ^R ; NSII targeting; PL _{lacO1} :: <i>nphT7</i> , <i>phaJ</i> , <i>phaB</i>	[42]
pDC304	Kan ^R ; NSII targeting; PL _{lacO1} :: <i>nphT7</i> , <i>yqhD</i> , synthetic RBS for <i>pduP</i> , <i>phaJ</i> , <i>phaB</i>	This work [45]

^a*nphT7* (*Streptomyces* sp. Strain CL190), acetoacetyl-CoA synthase; *bldh* (*C. saccharoperbutylacetonicum*), CoA-acylating butanal dehydrogenase; *yqhD* (*E. coli*), NADPH-dependent alcohol dehydrogenase; *phaJ* (*A. caviae*), (*R*)-specific crotonase; *phaB* (*R. eutropha*), acetoacetyl-CoA reductase; *pduP* (*S. enterica*), CoA-acylating propionaldehyde dehydrogenase; *ACCase* (*Yarrowia lipolytica*), acetyl-CoA carboxylase; Kan^R, kanamycin resistance; Gen^R, gentamycin resistance

2.2.2 Culture medium and growth conditions

All cyanobacterial strains were cultured at 30 °C, under constant illumination of 50 μmol photon m⁻²s⁻¹ in a temperature-controlled chamber. Liquid cultures were grown in modified BG-11 medium containing 50 mM NaHCO₃ in 300 mL screw cap flasks with continuous

shaking at 120 rpm as previously described [42]. In the case of mutants, 20 mg/L spectinomycin and 10 mg/L kanamycin were added to the medium. For pre-culture, a loopful of cells from solid medium were inoculated into a 20 mL liquid medium to an OD₇₃₀ of 1.5-2.0. For the main culture, cells were inoculated in a 50 mL BG-11 liquid medium with an initial density of OD₇₃₀ = 0.04. Feeding with 5 mL of fresh BG-11 medium containing 500 mM NaHCO₃ was done every 2 days until sampling time. IPTG and antibiotics were also added during feeding time.

2.2.3 Sampling and extraction

Sampling by fast filtration was done at 67 hours after IPTG induction as previously described [42]. Briefly, cell culture equivalent to 5 mg dry cell weight was filtered using a 0.2 µm pore size Omnipore membrane filter disc (Millipore, USA). Subsequently, the filtered cells were washed with pre-cooled 70 mM NH₄CO₃. The membrane filter containing the cells was placed on pre-chilled aluminum block to arrest cellular metabolic activity. Samples were stored in 15 mL centrifuge tubes at -80 °C until extraction.

Extraction of intracellular metabolites was done using the liquid-liquid extraction protocol with some modifications [33], [42]. One milliliter of mixed solvent (CH₃OH: CHCl₃:H₂O, 5:2:2, v/v) containing the internal standard (5 ppm of (+)-10-camphorsulfonic acid) was added to the sample tube. A freeze and thaw procedure consisting of incubation at -80°C for 1 h followed

by -30°C for 30 min was done. The sample tube was then mixed by vortex for 30sec and sonicated for 10 sec. This procedure was repeated two more times. Two milliliter of suspension was divided equally into 2 mL microfuge tubes and added with 200 μ L of water. Centrifugation at 10,000 g for 5 min at 4°C was performed to separate the polar and nonpolar phases. Eight hundred microliter of the resulting polar phase was transferred into a new 1.5 mL microfuge tube through filtering with a 0.20 μ m Millex-LG filter (Millipore, USA). To concentrate the samples, the filtered supernatant was subjected to centrifugal concentration for 2 h using a VC-96R Spin Dryer Standard (Taitec, Japan). Identical samples were then combined before overnight lyophilization in a VD-800F Freeze Dryer (Taitec, Japan). Lyophilized samples were stored at -80°C until LC/MS/MS analysis. In the case of extracellular metabolites extraction, 1 mL of culture medium was collected and centrifuged at 16,000 g for 5 min at 4 °C. The supernatant was transferred to a new 1.5 mL microfuge tube. Samples were stored at -30°C until GC/FID analysis.

2.2.4 Ion-pair reversed-phase LC/QqQ-MS analysis

The freeze-dried samples were dissolved in 30 μ L of ultrapure water for RP-IP-LC/QqQ-MS analysis using a Shimadzu Nexera UHPLC system coupled with LCMS 8030 plus (Shimadzu, Japan) with an L-column 2 ODS (150 mm \times 2.1 mm, 3 μ m, Chemicals Evaluation

and Research Institute, Japan) as previously described [21], [33], [34]. Analysis was performed using 10 mM tributylamine-15 mM acetic acid in water as mobile phase A and methanol as mobile phase B. The gradient concentration of the mobile phase with flow rate of 0.2 mL/min were as follows: start from 0% B at 0-1 min, increased to 15% B at 1.0 to 1.5 min, then held until 3.0 min, then increased to 50% and 100% B from 3.0 to 8.0 min, and 8.0 to 10.0 min, respectively; held 100% B until 11 min, decreased to 0% B from 11 to 11.50 min, and at last held 0% B until 17 min. The column oven temperature was 45 °C and the analysis mode was in negative ion mode. The mass spectrometer conditions were set at the following conditions: the desolvation line temperature was 250 °C, the nebulizer gas flow was 2 L/min, the drying gas flow was 15 L/min, and the heat block temperature was 400 °C and analysis mode was multiple reaction monitoring (MRM) mode (Table S1).

2.2.5 1-Butanol analysis

Alcohols were quantified by a GC-2010 system (Shimadzu, Japan) equipped with a flame ionization detector and an AOC-20i/s autoinjector (Shimadzu, Japan) using a GL Science Inert Cap Pure-WAX capillary column (30 m, 0.25 mm i.d., 0.25 µm film thickness). Isobutanol was added into the sample as an internal standard. The injector was maintained at 225°C. The column temperature was initially held at 40°C for 1 min and raised with a gradient of 15°C/min

until 120°C and held for 1 min, then raised with a gradient of 50°C/min until 250°C and held for 5 min. Nitrogen was used as the carrier gas with a column flow rate of 1.90 mL/min (linear velocity 40.0 cm/s).

2.2.6 Data analysis

The raw data set from LC/MS/MS analysis was converted to an analysis base file (.abf) format using a converter developed by Reifycs, Japan. MRMPROBS 2.19 [35] was used for peak picking and calculating the peak area. The detected peaks were also confirmed manually by using Lab solution (Shimadzu, Japan). Subsequently, the data matrix was subjected to multivariate analysis. To make the data easy to visualize, SIMCA-P+ version 13 (Umetrics, Sweden) was used for constructing the PCA (principal component analysis) plots. All data were standardized to autoscale: mean was 0, variance was 1. In addition, a student t-test analysis was performed using MS Excel to determine whether two sets of data were significantly different from each other.

2.2.7 PduP enzyme assay

Enzyme assays for PduP activity in the cyanobacterial crude extracts were performed as described in the previous work [19]. Cyanobacterial crude extracts were prepared by harvesting the fresh cultures after IPTG induction. The details of preparation of cell extract and the

incubation procedure have been described elsewhere [17]. A Bio-Tek Power-Wave XS microplate spectrophotometer was used to monitor the decrease of absorbance at 340nm, corresponding to the consumption of NADH. The reaction mixture contained 1mM dithiothreitol (DTT), 500 μ M NADH, 500 μ M butanoyl-CoA, and 50mM phosphate buffer (pH 7.15). The enzymatic reaction was started after the addition of the crude extract. (*PduP* enzyme assay was done in UCLA by collaborator, Derrick Chuang)

2.3 Results and discussion

2.3.1 Comparative metabolite analysis of EL22 and BUOHSE identified a possible target for strain improvement in 1-butanol biosynthesis

In this work, relative quantification approach for metabolomics was chosen over absolute quantification. It uses an internal standard to normalize the metabolite signal intensity. Since this procedure is experimentally less complicated and laborious, it allows for simultaneous profiling of a larger number of metabolites compared to absolute quantification, thereby broadening the metabolite coverage [31], [46]. By using ion-pair reversed phase liquid chromatography triple quadrupole mass spectrometer (IP-RP-LC/QqQ-MS) system, 74 metabolites (Table S2) belonging to the central metabolism of *Synechococcus elongatus* strains EL22 and BUOHSE were successfully annotated. In order to confirm that the previous target for strain improvement can also be detected by using widely targeted analysis, the data was initially compared to the absolute quantification data from previously published results [42]. As mentioned previously, quantitative target analysis of acyl-CoAs suggested the accumulation of butanoyl-CoA in BUOHSE as the target for strain improvement in 1-butanol biosynthesis. Thus, the relative concentration of butanoyl-CoA in BUOHSE in comparison with EL22 was investigated. As shown in figure 2.3-1, the results also showed comparable levels of butanoyl-CoA in EL22 and BUOHSE, illustrating a good agreement with the previous study [42].

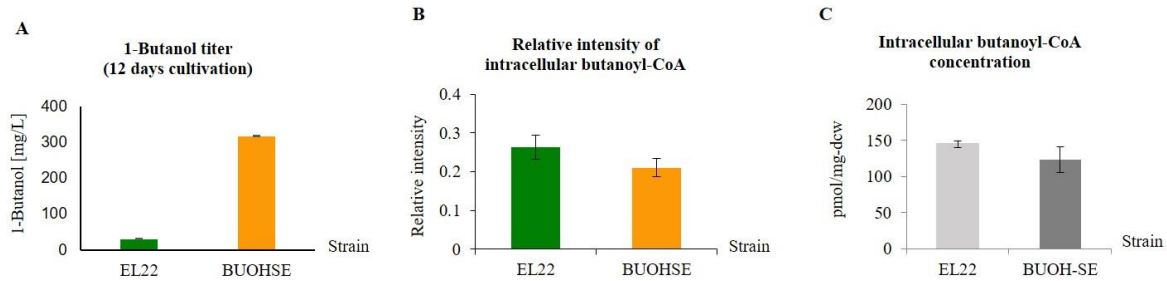


Figure 2.3-1. (A) In-flask 1-butanol titers from EL22 and BUOHSE. Samples were taken 12 days after IPTG induction under light and aerobic conditions. (B) Relative intensity of intracellular butanoyl-CoA measurements from widely targeted metabolic profiling of EL22 and BUOHSE. The y-axis represents the relative intensity of the metabolites, which was normalized to an internal standard. (C) Absolute intracellular concentration of butanoyl-CoA (pmol/mg-dry cell weight (dcw)) in EL22 and BUOHSE [42]. Samples were taken 67 hours after IPTG induction. The error bars indicate standard deviations obtained from three replicates.

Subsequently, I then employed Principle Component Analysis (PCA) to analyze which of the 74 annotated metabolites exhibited the most significant difference between the two strains.

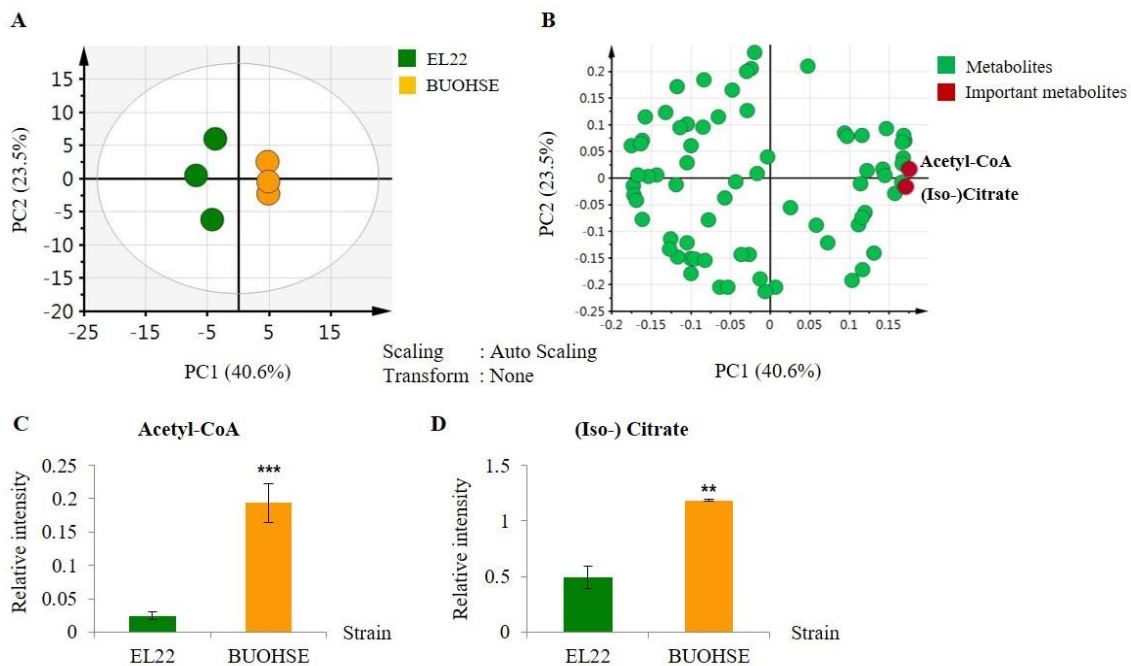


Figure 2.3-2. (A) PCA score plot showing clear distinction between EL22 (in green circles) and BUOHSE (in yellow circles). (B) Loading scatter plot indicating metabolites that have influence on the clustering of the score plot. Relative intensity of two important metabolites: (C) acetyl-CoA and (D) (iso-) citrate. (Iso-) Citrate in this study refers to iso-citrate and citrate as it is not possible to separate the two metabolites in our system. The y-axis represents the unit for the relative intensity of metabolites, which was normalized to an internal standard. Asterisks indicate significant differences in the strains (**: $p \leq 0.01$; ***: $p \leq 0.001$). All error bars indicate standard deviations obtained from three replicates.

Principal component analysis (PCA) is a well-known statistical technique used to determine variation and highlight important patterns in a dataset [47]. The correlations between observations and its variables are easily seen by using this multivariate analysis. From the PCA score plots (Fig. 2.3-2A), a distinct separation of EL22 and BUOHSE along the first principal component (PC1) was observed. PC1 represented 40.6% of the total variance of the samples, while PC2 was 23.5%. Furthermore, to evaluate which metabolites that give contribution in discriminating EL22 and BUOHSE, PCA loading plot and student t-test were carried out. First, visual inspection of the loading plot obtained from PCA analysis was performed. The PCA loading plot showed that tricarboxylic acid (TCA) cycle-related compounds such as acetyl-CoA and (iso-) citrate gave the most contribution for discriminating between the two strains (Fig. 2.3-2B). Moreover, to investigate the contribution of other metabolites, metabolites with the most positive or most negative along the PC1 was then tested to check for significant difference. I performed student t-test to examine the significant difference of metabolites between the

samples. The cut off p-value was set to 5%. The asterisks mark follows this rule: *: $p \leq 0.05$;

: $p \leq 0.01$; *: $p \leq 0.005$. Metabolites which have significant values are then further observed.

Table below are the list of metabolites that are significantly different among the samples.

Table 2.3-1. Highly significant metabolites based on student t-test of EL22 in comparison with BUOHSE

Metabolites	p-value	Mark
Acetyl-CoA	0.000617	***
Glutathione	0.003858	***
FMN	0.004659	***
ATP	0.005748	**
Glycolate	0.006349	**
Iso-/Citrate	0.006452	**
Tyrosine	0.006591	**
Arginine	0.007244	**
Valine	0.015912	**
Cysteine	0.016326	*
Phenylalanine	0.016562	*
Aspartate	0.018900	*
TMP	0.023702	*
Thymidine	0.024176	*
UDP-Glucose	0.031035	*
CTP	0.032989	*
SBP	0.034684	*
IMP	0.034977	*
Tryptophan	0.036269	*

Among the significantly different metabolites based on multivariate (PCA) and univariate analysis (student t-test), metabolites that are closely associated with CoA-dependent pathway were first selected. This is because the metabolites closely related to CoA-dependent may have direct effect for 1-butanol improvement. In case of comparison between EL22 and BUOHSE, acetyl-CoA, a precursor for the CoA-dependent pathway, is shown to be the most positively contributing metabolite to the separation of the two strains in PCA and has the lowest p-value. Subsequently to learn the trend, other metabolites that are associated with acetyl-CoA among the metabolites that are significantly different between the two strains were examined. Iso-/citrate was found to give high contribution to the separation in the PCA and has low p-value. Therefore, acetyl-CoA and (iso-) citrate are considered as important metabolites and can be used as a clue for strain improvement.

In addition to that relative intensity of acetyl-CoA and (iso-) citrate was then investigated in order to get a better illustration. Results indicated that acetyl-CoA (Fig. 2.3-2C) and (iso-) citrate (Fig. 2.3-2D) accumulated in BUOHSE compared to EL22. Significantly higher level of acetyl-CoA in BUOHSE compared to EL22 possibly occurred due to an increasing rate of acetyl-CoA synthesis, as explained in the previous work [42]. From the reduction reaction of butanoyl-CoA to butanal free CoA was regenerated. This free CoA regeneration may play a role to supply free CoA for the conversion of pyruvate to acetyl-CoA. In the acetyl-CoA

biosynthesis via pyruvate, not only the supply of free CoA but also availability of NAD^+ is important to facilitate the reaction. Since Bldh enzyme that catalyzed butanoyl-CoA to butanal in EL22 is NAD(P)H-dependent, there was a possibility that the insufficient NAD^+ pool was the limiting factor in converting pyruvate to acetyl-CoA via pyruvate dehydrogenase complex (PDH). However, previous work [42] result showed that the intracellular NAD^+ concentration of EL22 was slightly higher than that of BUOHSE. This suggested that the intracellular NAD^+ concentration of strain EL22 is enough to convert pyruvate to acetyl-CoA via PDH. Thus, it was assumed that increasing level of acetyl-CoA in BUOHSE was occurred due to more effective regeneration of free CoA from butanoyl-CoA via the reductive reaction catalyzed by PduP.

To further validate this phenomenon, a widely targeted metabolome analysis of BUOHSE strain without *pduP* in comparison with BUOHSE strain was carried out. Results showed that the relative intensity of acetyl-CoA (Fig. 2.3-3B) and (iso-) citrate (Fig. 2.3-3C) in BUOHSE strain without *pduP* were significantly lower compared to BUOHSE, while butanoyl-CoA was significantly higher (Fig. 2.3-3A). This suggested that without *pduP*, the conversion of butanoyl-CoA to butanal was hampered thus leading to the decrease in acetyl-CoA synthesis and (iso-) citrate formation.

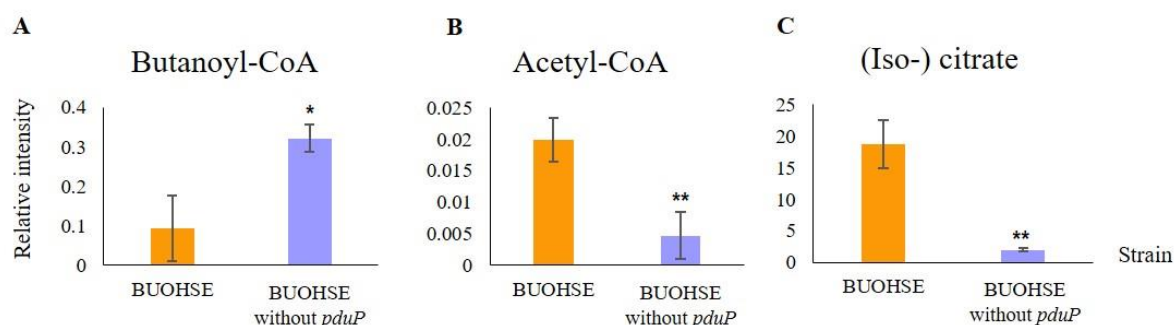


Figure 2.3-3. Relative intensity of intracellular (A) butanoyl-CoA, (B) acetyl-CoA, and (C) (iso-) citrate in BUOHSE and BUOHSE without *pduP*. Asterisks indicate significant differences in the strains (*: $p \leq 0.05$; **: $p \leq 0.01$).

Hence, PduP is predicted to not only play a vital role in the conversion of butanoyl-CoA to butanal but also in free CoA regeneration, which is required for the function of the 1-butanol pathway. Therefore, this study also suggested that the improvement of PduP enzyme may be useful for enhancing 1-butanol production. In addition, the higher level of (iso-) citrate observed in BUOHSE compared to EL22 indicated the possibility that the accumulated acetyl-CoA was used for the TCA cycle instead of the CoA-dependent 1-butanol pathway. Thus, diverting the increased acetyl-CoA pool towards the CoA-dependent 1-butanol pathway by improving the reaction from acetyl-CoA to malonyl-CoA seems to be a promising strategy for strain improvement.

2.3.2 Enhancing 1-butanol titers by improving PduP enzyme activity

To improve the reaction from butanoyl-CoA to butanal, PduP activity was improved in the BUOHSE background strain to generate strain DC7 (Fig. 1.3-1). Salis RBS calculator [48] is a useful tool for allowing modulation of RBS strength in various model organisms in order to control protein expression. In this study, it was used to design different RBS sequences to replace the original RBS upstream of *pduP* on the plasmid pSR3 (Fig. 2.3-4).

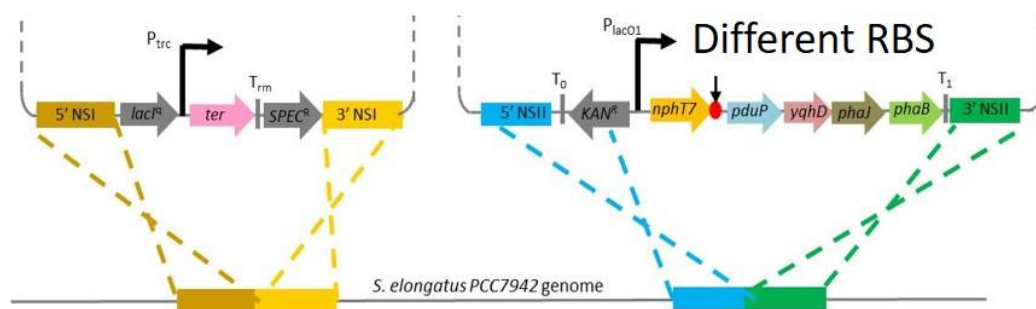


Figure 2.3-4. Schematic of strategy to replace the original ribosome binding site (RBS) upstream of *pduP* with synthetic RBS

Among several newly-constructed strains, 1-butanol production in DC7 outperformed the published strain BUOHSE [19] by 33% with a final titer of 426.75mg/L in 12 days after IPTG induction (Fig. 2.3-5). Specific enzyme activity in the crude extract was measured to validate if the PduP activity was in fact increased in DC7. A 1.4 folds increase in the PduP enzyme activity was observed in DC7 compared to BUOHSE (Fig. 2.3-5C). Furthermore, a significant decrease in intracellular butanoyl-CoA was also detected (Fig. 2.3-5B). Taken together, these results

indicated that optimization of PduP activity effectively led to an improved conversion of butanoyl-CoA into butanal, further increasing 1-butanol titer in DC7. Moreover, Salis RBS Calculator has proven to be a valuable tool in this work, and it has functioned as intended.

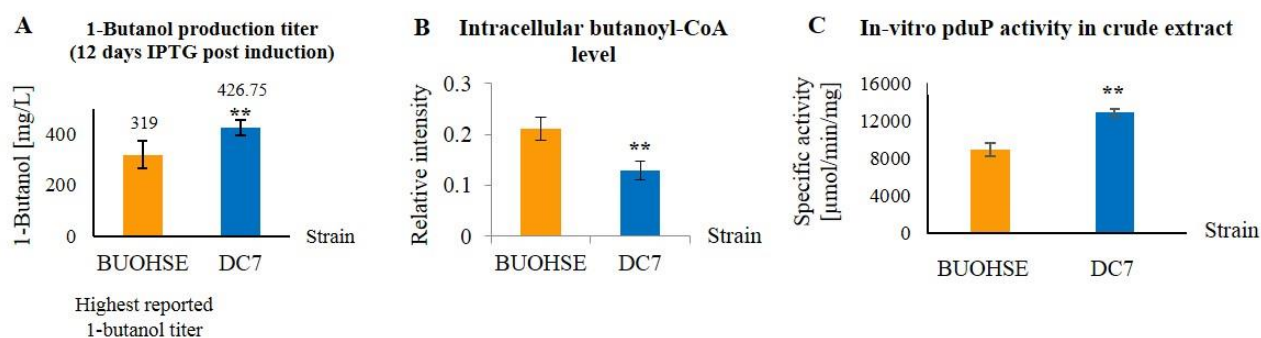


Figure 2.3-5. (A) In-flask 1-butanol titers from BUOHSE and DC7. Samples were taken 12 days after IPTG induction under light and aerobic conditions. (B) Relative intensity of intracellular butanoyl-CoA measurements in BUOHSE and DC7. (C) In -vitro specific activity of PduP in crude extract of BUOHSE and DC7 (*PduP enzyme activity work was done by collaborator*). Asterisks indicate significant differences in the strains (**: $p \leq 0.01$). The error bars indicate standard deviations obtained from three replicates.

Chapter 3

Optimization of acetyl-CoA to malonyl-CoA reaction enables high titer and productivity of 1-butanol

3.1 Introduction

In Chapter 2, the previously suggested possible target for strain improvement in CoA-dependent pathway of *S. elongatus* 1-butanol producing strain [42], butanoyl-CoA to butanal reaction which is catalyzed by PduP enzyme, was validated and successfully solved. By replacing the original RBS with synthetic RBS upstream of pduP in BUOHSE, the new strain DC7 was generated. The DC7 strain successfully exceeded the highest recorded 1-butanol titer (317 mg/L) [19] that was achieved in BUOHSE by 33% (426.75 mg/L) (Fig. 2.3-5A). Additionally, to confirm that the increasing 1-butanol titer was caused by the RBS modification, butanoyl-CoA level in DC7 was further investigated and specific activity of PduP enzyme in the crude extract was measured. Results showed that butanoyl-CoA level decreased significantly and a 1.4 fold increase in PduP enzyme activity was observed in DC7 compared to BUOHSE (Fig. 2.3-5B, 5C). This validated that the metabolomics insight could help to effectively find specific target for strain improvement and that RBS modification upstream of *pduP* in CoA-dependent pathway led to increase in titer of 1-butanol.

For bioproduction that involves industrial microorganisms, production titer and production rate are phenotypes that should be targeted for improvement. Therefore, comparative metabolome analysis of BUOHSE and DC7 was carried out in Chapter 3 to understand the effect of PduP optimization and to seek a new possible target in attempt to improve the production rate. The data suggested that acetyl-CoA and (iso-) citrate was highly accumulated in DC7 strain compared to BUOHSE. Briefly, this accumulation suggested that acetyl-CoA to malonyl-CoA reaction could be considered as a new target in the CoA-dependent pathway. Furthermore, based on the results, TCA cycle was assumed to be a competing pathway for 1-butanol formation. In order to maximize production of 1-butanol, it is desirable to ensure that the available precursors can be channeled into the biosynthetic pathway. Therefore, by preventing available precursors to go enter competing pathways (in this case the TCA cycle), improved production can likely be seen. Hence, acetyl-CoA carboxylase (ACCase), enzyme that catalyzes acetyl-CoA to malonyl-CoA reaction, was selected as the next target in this second round of strain improvement. Genetic modification involved two main strategies: 1) disruption of *aldA* gene, encoding for alcohol dehydrogenase, to eliminate any unwanted consumption of acetyl-CoA and 2) introduction of *accase* gene from *Yarrowia lipolytica* into the disruption site. By using this engineering strategy, high productivity was successfully

achieved in the newly constructed strain DC11 which outperformed the first reported high 1-butanol producing strain BUOHSE by 57% (74.5 mg/L per day) (Lan et al. 2013b).

3.2 Materials and methods

3.2.1 Cyanobacterial strains and plasmids

Strains and plasmids used in the Chapter 3 are listed in Table 3.2-1. DC7 strain construction was previously described in section 2.2.1. For the newly constructed strain DC11, plasmid pDC331 encoded by *accase* gene from *Yarrowia lipolytica* was introduced in strain DC7 into the *aldA* site and the DC11 was then selected by 5µg/ml gentamicin on the plates. Full segregation of each strain was verified through PCR (Fig. S1). (*Strain construction was done in UCLA by collaborator, Derrick Chuang*)

Table 3.2-1. Strains and plasmids used in this study^a

Cyanobacteria strain	Genotype	Reference
BUOHSE	P _{Trc} :: His-tagged <i>T. denticola ter</i> integrated at NSI and PL _{lacO1} :: <i>nphT7</i> , <i>pduP_S. enterica</i> , <i>yqhD</i> , <i>phaJ</i> , <i>phaB</i> integrated at NSII	[19]
DC7	P _{Trc} :: His-tagged <i>T. denticola ter</i> integrated at NSI and PL _{lacO1} :: <i>nphT7</i> , <i>PduP_S. enterica</i> , <i>yqhD</i> , <i>phaJ</i> , <i>phaB</i> integrated at NSII, synthetic RBS TIR: 522266.72 in front of <i>pduP</i>	This work [45]

DC11	P _{Trc} :: His-tagged <i>T. denticola ter</i> integrated at NSI and PL _{lacO1} :: <i>nphT7</i> , <i>pduP</i> <i>S. enterica</i> , <i>yqhD</i> , <i>phaJ</i> , <i>phaB</i> integrated at NSII, synthetic RBS TIR: 522266.72 in front of <i>pduP</i> PL _{lacO1} : <i>ACCCase</i> integrated at <i>aldA</i>	This work [45]
Plasmid	Genotype characteristic	Reference
pSR3	Kan ^R ; NSII targeting; PL _{lacO1} :: <i>nphT7</i> , <i>yqhD</i> , <i>pduP</i> , <i>phaJ</i> , <i>phaB</i>	[19]
pDC304	Kan ^R ; NSII targeting; PL _{lacO1} :: <i>nphT7</i> , <i>yqhD</i> , synthetic RBS for <i>pduP</i> , <i>phaJ</i> , <i>phaB</i>	This work [45]
pDC331	Gen ^R ; <i>aldA</i> targeting; PL _{lacO1} : <i>ACCCase</i> <i>Yarrowia lipolytica</i> integrated at <i>aldA</i>	This work [45]

^a*nphT7* (*Streptomyces* sp. Strain CL190), acetoacetyl-CoA synthase; CoA-acylating butanal dehydrogenase; *yqhD* (*E. coli*), NADPH-dependent alcohol dehydrogenase; *phaJ* (*A. caviae*), (*R*)-specific crotonase; *phaB* (*R. eutropha*), acetoacetyl-CoA reductase; *pduP* (*S. enterica*), CoA-acylating propionaldehyde dehydrogenase; *ACCCase* (*Yarrowia lipolytica*), acetyl-CoA carboxylase; Kan^R, kanamycin resistance; Gen^R, gentamycin resistance

3.2.2 Culture medium and growth conditions

Cultivation were performed in the same procedures as described in section 2.2.2

3.2.3 Sampling and extraction

Sampling and extraction was performed with the same protocol as described in section 2.2.3

3.2.3 Absolute quantification of CoA-related metabolites

The intracellular concentration of CoA, acetyl-CoA, and butanoyl-CoA was determined using ^{13}C -isotope labelling experiment following the protocol used in the previous study with minor modifications. [42]. Fully ^{13}C -labeled cell extracts of BUOHSE and DC7 strains were prepared. Cells were cultivated as described previously except that $\text{NaH}^{13}\text{CO}_3$ (>98 atom % ^{13}C , Cambridge Isotope Laboratories, USA) was used instead of NaHCO_3 . Sampling was performed 3 days after IPTG induction in the same way as described above except that pre-cooled deionized water was used as washing solvent instead of NH_4CO_3 . Cells were extracted as described above except without the freeze-drying step. Extraction was repeatedly conducted for four times. After samples were concentrated for 2 hours using centrifugal concentration, all samples were combined in a 15 mL centrifuge tube. This ^{13}C -labelled cell extract was used as an internal standard. Six point calibration curve was constructed for each metabolite using peak area ratios of $\text{U-}^{12}\text{C}$ to $\text{U-}^{13}\text{C}$, as described previously [42]. The detailed description of calibration curve for each metabolite is listed in Table S3. Analysis mode was multiple reaction monitoring (MRM) mode in IP-RP-LC/QqQ-MS system (Table S4).

3.2.4 Ion-pair Reversed-Phase LC/QqQ-MS analysis

Metabolites were analyzed as described in section 2.2.4.

3.2.5 1-Butanol analysis

1-Butanol concentrations were quantified with the same procedure as described in section 2.2.5

3.2.6 Data analysis

The obtained results were analyzed with the same procedure as described in section 2.2.6.

3.2.7 RNA extraction and *Reverse Transcription* Polymerase Chain Reaction (RT-PCR)

Strain DC11 grown in BG11 with 50mM sodium bicarbonate under light condition($50\mu\text{E}/\text{m}^2\text{s}$) was induced by 1mM IPTG when OD_{730} reached between 0.4 to 0.6. The cultures were harvested 24 hours after IPTG induction. The total RNA was extracted by using the RiboPure RNA Purification kit (Invitrogen), following the manufacturers' protocol. The isolated RNA was further treated with DNase I (Invitrogen) for 30 minutes at 37°C. The reagents for reverse transcription PCR was performed by using the iTaq Universal SYBR Green One-Step kit (BIO-RAD). The primers for the RT-PCR were designed by the NCBI/Primer-Blast tools. The forward primer 5'-GGAATCGCTAGTAATCGCA-3' and reverse primer 5'-GCTACCTTGTTACGACTTCA-3' were used to amplify 16S rRNA as a control. The forward

primer 5'-TTGTCACCACTGAGATTGAG-3' and the reverse primer 5'-TATCCTTGTAGGCTCGAGAA-3' were used to amplify the heterologous *acetyl-CoA carboxylase (accase)* from *Yarrowia lipolytica*. RT-PCR was conducted by the following condition: 50°C for 10 min, 95°C for 1 min, 40 cycles of 95°C for 10 s and 60°C for 30 s. The melting curve was obtained from 65°C to 95°C by the increase of 0.5°C. The cycle threshold (C_t) value was acquired and analyzed by the CFX Manager software (BIO-RAD). (*RT-PCR experiment was done in UCLA by collaborator, Derrick Chuang*)

3.3 Results and discussion

3.3.1 Characterization of DC7 strain by widely targeted metabolic profiling

To gain a deeper understanding of the overall effect of the increased PduP activity in DC7 and to identify other targets for strain engineering, I applied the same widely targeted metabolic profiling strategy to compare BUOHSE and DC7. Based on PCA analysis, acetyl-CoA and (iso-) citrate were found to be important metabolites for discriminating the two strains (Fig. 3.3-1A). Specifically, DC7 showed increased levels of acetyl-CoA and (iso-) citrate compared to BUOHSE (Fig. 3.3-1B). Interestingly, this result showed a similar tendency when EL22 and BUOHSE were compared, which also showed increased acetyl-CoA and (iso-) citrate (Fig. 2.3-

2C, 2D). This also suggested that an increase in free CoA regeneration upon improvement of the PduP enzyme led to a higher accumulation of acetyl-CoA in DC7 (Fig. 3.3-1B, Fig. 3.3-2). Moreover, the enhanced level of (iso-) citrate in DC7 in comparison to BUOHSE strengthen the hypothesis generated from comparing EL22 and BUOHSE. It indicated that carbon from acetyl-CoA may be entering into the TCA cycle, which in turn may act as a drain of this 1-butanol precursor (Fig 3.3-2).

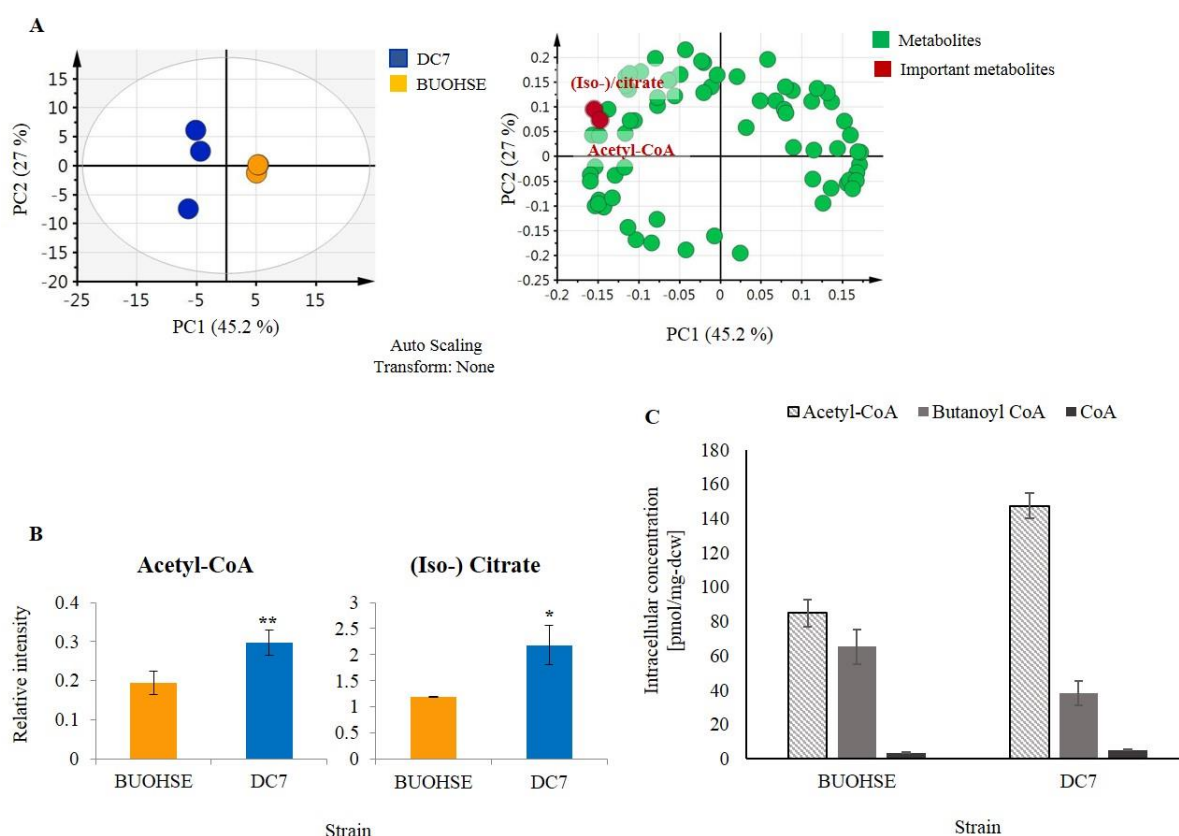


Figure 3.3-1. (A) PCA score plot and loading plot derived from metabolic profiling of BUOHSE and DC7. The score plot showed distinct separation of DC7 and BUOHSE, represented by blue and yellow circles, respectively. The loading plot revealed good correlation

of acetyl-CoA and (iso-) citrate with the DC7 data set. (B) Relative intensity of intracellular acetyl-CoA and (iso-) citrate levels in BUOHSE and DC7. Asterisks indicate significant differences in the strains (*: $p \leq 0.05$; **: $p \leq 0.01$). (C) Intracellular concentration of acetyl-CoA, butanoyl-CoA and free CoA in BUOHSE and DC7. The error bars indicate standard deviation obtained from three replicates.

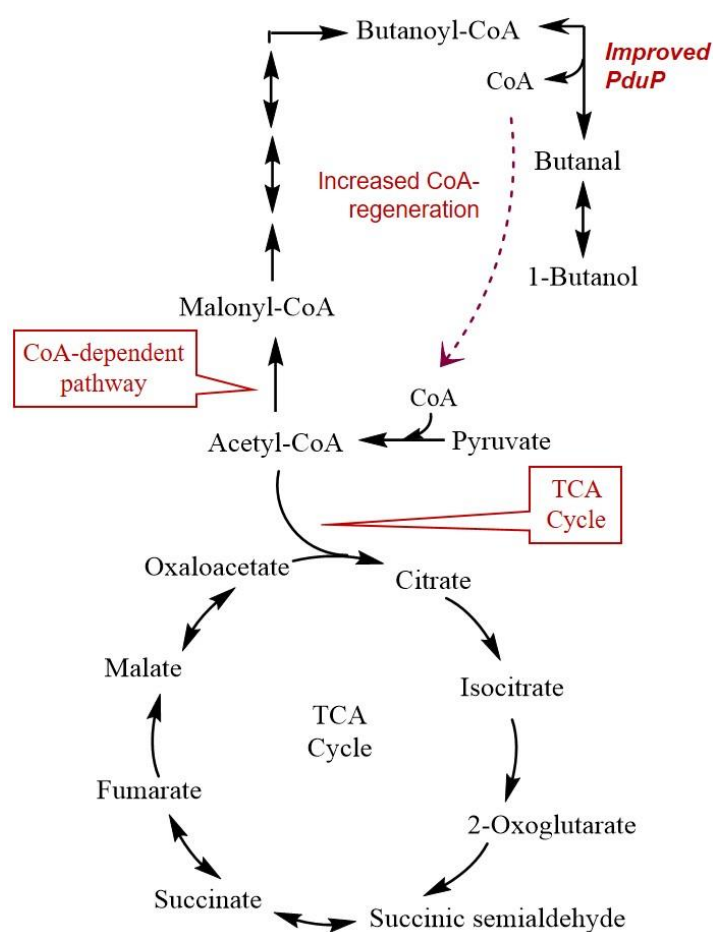


Figure 3.3-2. Schematic representation of 1-butanol biosynthesis pathway and TCA cycle.

Since relative quantification indicates concentration relative to the internal standard, this method cannot be used for comparison of different metabolites within one strain. Hence, it could not be concluded whether the reaction to convert the accumulated acetyl-CoA to 1-butanol is a

logical target for improvement as the concentration of acetyl-CoA cannot be compared to other CoA metabolites. Therefore, to know the absolute concentration of acetyl-CoA in comparison to other acyl-CoA metabolites, absolute quantification was carried out. Quantification of the absolute concentration of CoA-dependent pathway-related metabolites in the DC7 was performed by using ^{13}C -labelled cyanobacterial cell extract as internal standard. Result showed that acetyl-CoA concentration was highly accumulated in the DC7 strain compared to other CoA-related metabolites (Fig. 3.3-1C). Thus, by diverting more acetyl-CoA into CoA-dependent pathway, further improvement of 1-butanol production might be achieved.

In addition to the PCA analysis, based on the student t-test, some metabolites that are not closely related to CoA-dependent pathway, such as 3PGA, R5P, Ru5P, PEP and UDP-Glucose (upstream metabolites), were also found to have high significant values in discriminating BUOHSE and DC7 (Table 3.3-1). However, in this study, acetyl-CoA was selected as first target for strain improvement since it is directly related to the production pathway. Nevertheless, the finding of other metabolites might be useful for future study to further improve 1-butanol in engineered cyanobacteria. The study carried out by Nishiguchi, 2019 [22] using ensemble kinetic modelling analysis, described that 3-phosphoglycerate (3PGA) has a large pool size in *S. elongatus* ethanol producing strain. Overexpression of PGK (phosphoglycerate kinase) successfully improved ethanol titers by up to 1.37 fold compared to the control strain. Thus,

this finding may also be applicable for 1-butanol improvement in engineered cyanobacteria.

However, further analysis related to this hypothesis is necessary.

Table 3.3-1. Highly significant metabolites based on t-test of BUOHSE in comparison with DC7

Metabolites	p-value	Mark
CMP	0.000107	***
3PGA	0.000224	***
Cysteine	0.001229	***
PEP	0.001394	***
Tyrosine	0.001747	***
UDP-Glucose	0.002892	***
Arginine	0.003641	***
CDP	0.006011	**
Glycolate	0.008056	**
Butanoyl-CoA	0.008176	**
Valine	0.009892	**
R5P	0.011651	**
Ru5P	0.012633	**
Acetyl-CoA	0.015169	**
Disaccharide-P	0.016368	*
AMP	0.020683	*
UMP	0.033502	*
SBP	0.036914	*
Iso-/Citrate	0.045867	*
Histidine	0.046973	*

3.3.2 Optimization of ACCase enzyme to divert enhanced level of acetyl-CoA towards 1-butanol formation

Carboxylation reaction of acetyl-CoA to malonyl-CoA is the direct downstream reaction of acetyl-CoA in the 1-butanol pathway and is catalyzed by the native ACCase complex [49]. This reaction serves as an essential component to many biosynthetic pathways [50], and is a notorious bottleneck in the production of a diverse set of compounds [51]. Therefore, as the next strategy for strain improvement, I focused on this reaction in order to enhance acetyl-CoA utilization. Modifications on the ACCase enzyme were carried out using DC7 as background strain. The ACCase enzyme in cyanobacteria, similar to majority of higher plants, is composed of multiple identical subunits [49], [52]. This complex structure of ACCase makes this enzyme difficult to modify or overexpress. However, several reports in *Yarrowia lipolytica* (*Y. lipolytica*) demonstrated the successful overexpression of a single subunit of ACCase for improvement of fuel-like molecules and oleochemicals production [53]–[56]. Moreover, several studies on the overexpression of ACCase in various microorganisms, such as *Escherichia coli* [57] and *Saccharomyces cerevisiae* [58] for production of valuable compounds, have also been published. Nevertheless, no studies have been reported on *Synechococcus elongatus*. Therefore, we attempted to increase the activity of ACCase by inserting a single subunit of *accase* gene from *Y. lipolytica* into the *aldA* site. In *Synechococcus elongatus*

PCC7942, *aldA* encodes for alcohol dehydrogenase [54] that converts acetyl-CoA to acetaldehyde hence, disrupting this gene might also help to eliminate any unwanted consumption of acetyl-CoA (Fig. 3.3-3).

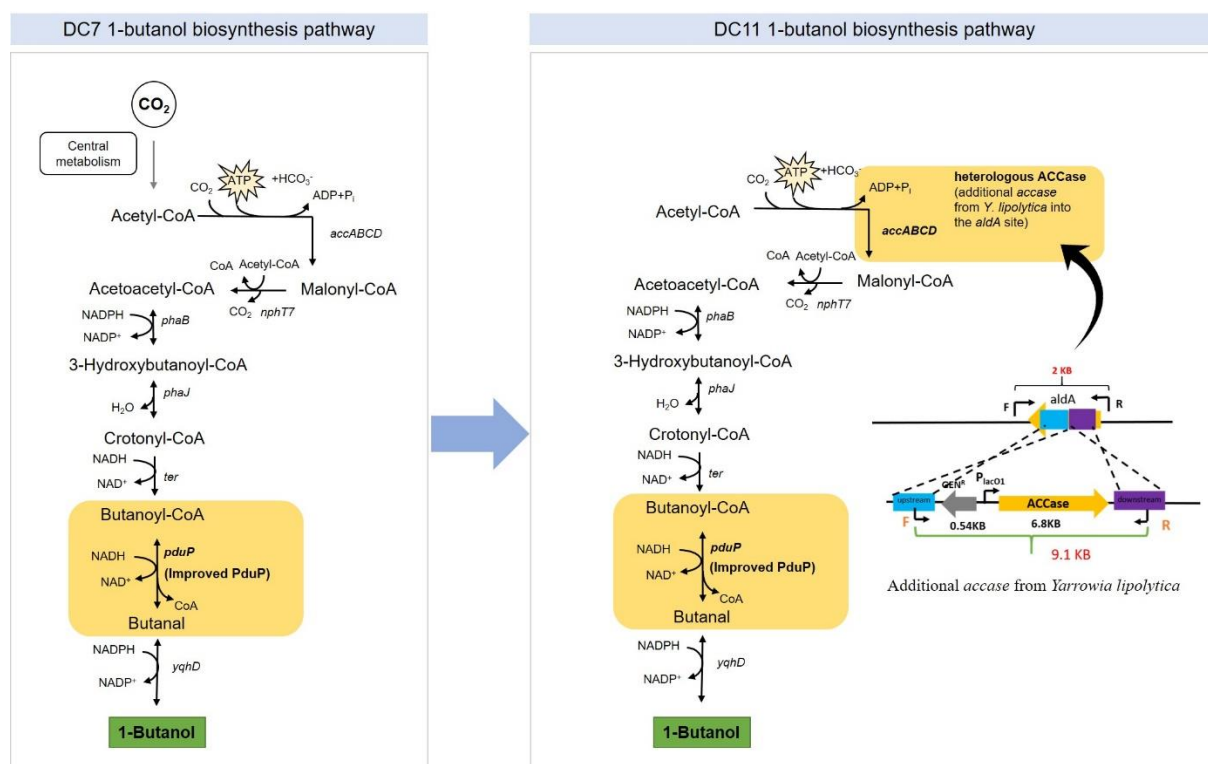


Figure 3.3-3. Schematic of genetic modification in synthetic 1-butanol biosynthesis pathway of DC7 and DC11.

Based on this strategy, result showed that the DC11 strain (Fig. 2D), which contains *accase* from *Yarrowia lipolytica*, was able to reach a production titer of 418.7 mg/L in 6 days, while DC7 strain can reach a similar titer in 12 days (Fig. 3.3-4A). This modification successfully achieved a maximum 1-butanol titer of 117 mg/L per day between days 4 and 5 (Fig. 3.3-4C), 57% higher compared to the best 1-butanol producing strain BUOHSE (74.5 mg/L per day) that

was previously reported. Specifically, 1-butanol productivity of DC11 on day 4 and 5 was increased by 1.48 and 1.41 fold compared to BUOHSE, respectively (Fig. 3.3-4D).

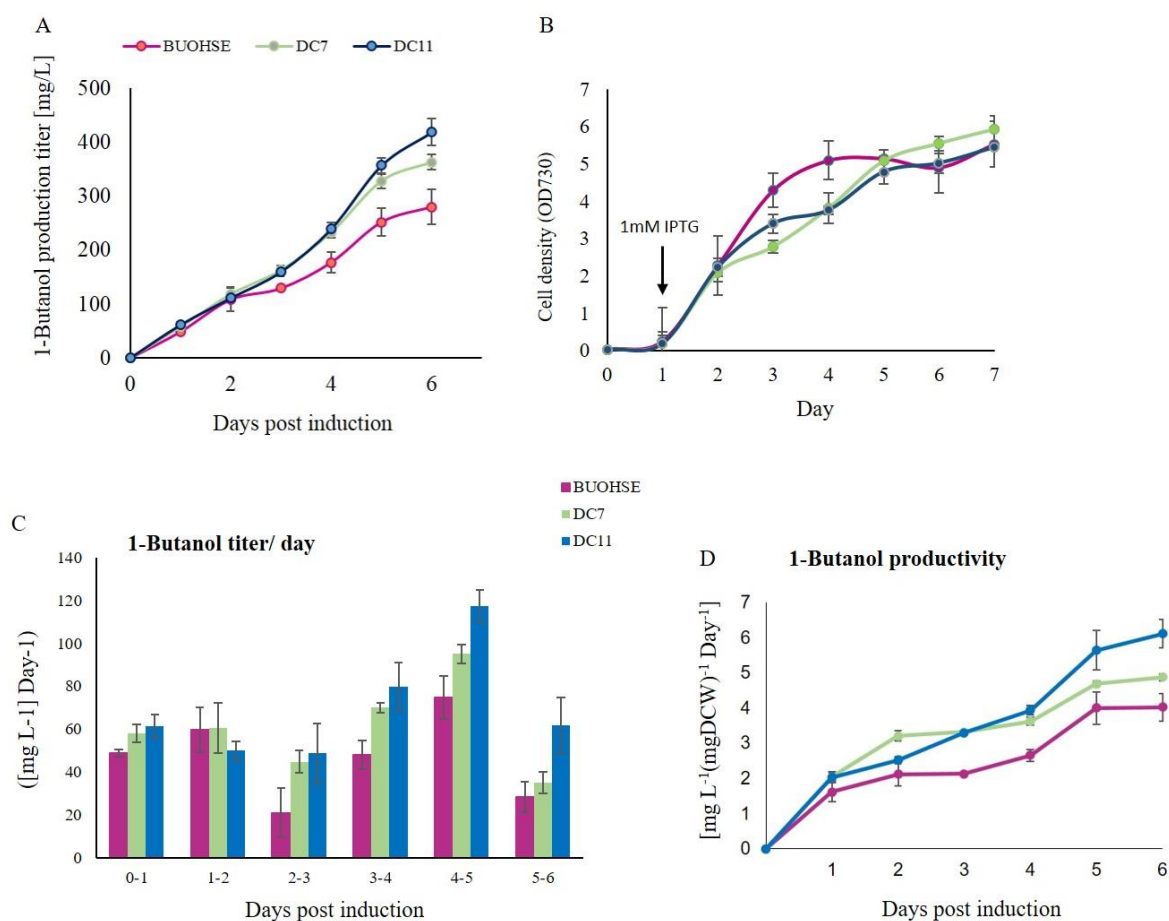


Figure 3.3-4. (A) 1-Butanol production of *S. elongatus* BUOHSE, DC7, and DC11 strains. (B) Daily titer of 1-butanol by *S. elongatus* BUOHSE, DC7, and DC11 strains. (C) Cell density of *S. elongatus* BUOHSE, DC7, and DC11 strains. (D) 1-Butanol productivity. The error bars indicate standard deviations obtained from three replicates.

3.3.2 Characterization of DC11 strain by LC/MS/MS system

To gain further insight into the metabolic perturbations that resulted from this modification, widely targeted metabolomics to compare DC7 and DC11 strains was employed. PCA results showed that CoA-related metabolites, amino acids, and sugars have a positive contribution in the separation of DC11 strain from DC7 strain (Fig. 3.3-5A). Since DC11 was developed from the DC7 strain, PduP enzyme profile for both strains was expected to be the same. Therefore, a comparable level of butanoyl-CoA in DC11 and DC7 was reasonably observed (Fig. 3.3-5C). Among the measured metabolites, malonyl-CoA showed a drastic increase in DC11 (Fig. 3.3-5C) thereby validating that the insertion of *accase* gene from *Y. lipolytica* was able to increase the ACCase activity. In addition, since there is no reliable assay platform to detect the activity of ACCase in crude extracts, we alternatively used *reverse transcription* polymerase chain reaction (RT-PCR) to confirm that the single unit of ACCase from *Y. lipolytica* was indeed transcribed in *S. elongatus* PCC7942 (Fig. 3.3-5D). However, in the metabolome data, a significant change in acetyl-CoA concentration or (iso-) citrate concentration could not be observed (Fig. 3.3-5C). Acetyl-CoA pool is highly dynamic and can be affected by other factors, such as increasing rate of CoA recycling upon PduP improvement which resulted in an enhanced rate of acetyl-CoA synthesis that was previously mentioned in the previous study [42]. Moreover, simultaneous deletion of *aldA* may also aid in preventing acetyl-CoA degradation.

Therefore, improvement of both ACCase and PduP in DC11 may conceivably improve the overall pathway leading to 1-butanol production.

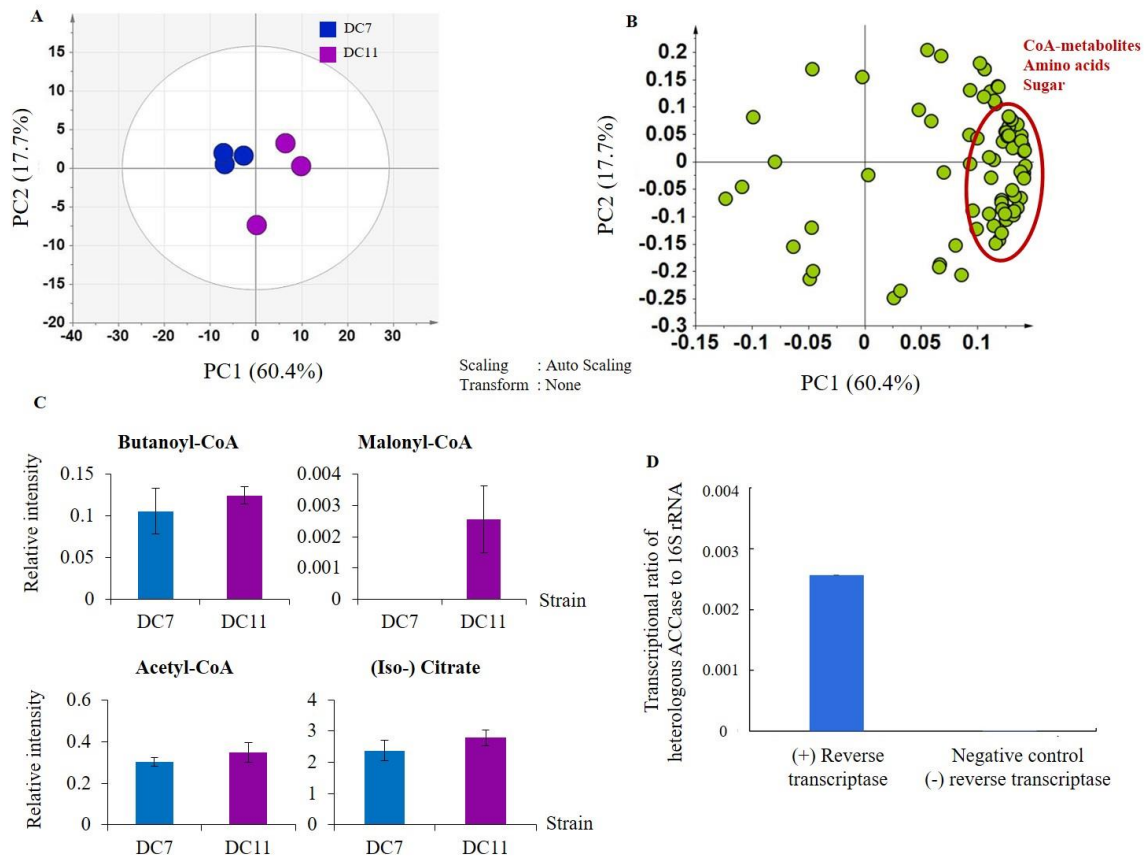


Figure 3.3-5. (A) PCA score plot and loading plot derived from DC7 and DC11. The score plot showed distinct separation of DC7 and DC11, represented by respective blue and purple circles. (B) The loading plot revealed CoA-dependent pathway-related metabolites, amino acids, and sugars had a positive contribution for separating DC11 with DC7. (C) Relative intensity of intracellular butanoyl-CoA, malonyl-CoA, acetyl-CoA and (iso-) citrate in DC7 and DC11. Asterisks indicate significant differences in the strains (*: $p \leq 0.05$; **: $p \leq 0.01$). (D) RT-PCR for heterologous *accase* expressed in *S. elongatus* PCC7942 (*RT-PCR work was done by collaborator*).

Chapter 4

Conclusions and future perspectives

In this study, metabolic profiling using LC/MS/MS system was used to investigate the metabolic response of different gene modifications and to identify the target for future strain improvement in the CoA-dependent pathway. After modification of the pathway based on metabolomics insights, the highest reported 1-butanol titer and productivity for engineered *Synechococcus elongatus* PCC 7942 was successfully achieved. In particular, widely targeted metabolic profiling of EL22 and BUOHSE successfully confirmed that the reduction reaction from butanoyl-CoA to butanal, catalyzed by PduP enzyme, was the target that needed to be improved in the CoA-dependent 1-butanol pathway. Thus, by increasing PduP activity, the newly generated strain DC7 was able to increase 1-butanol production by 33% compared to BUOHSE (the previously reported best 1-butanol producing strain). Moreover, the metabolome analysis also suggested that acetyl-CoA was highly accumulated upon PduP enzyme modification. Thus, ACCase enzyme, catalyzing the reaction of acetyl-CoA to malonyl-CoA, was selected as a new target for second round of strain improvement. Hence, by increasing the activity of ACCase enzyme through the insertion of *accase* from *Yarrowia lipolytica* in the DC7

strain, an increase in 1-butanol productivity (DC11 strain) was achieved. The DC11 strain reached a production titer of 418.7 mg/L in 6 days, while DC7 reached a similar titer in 12 days.

To date, this is the first report of the integration of *accase* gene from eukaryotic single-cell, *Y. lipolytica*, in the unicellular cyanobacterium, *S. elongatus* 1-butanol producing strain. As a matter of fact, advancement of genome engineering in cyanobacteria is far behind well-studied model microorganisms [59]. Thus, this study also gave new insight on genetic engineering strategy in cyanobacterium *S. elongatus* PCC 7942. Through the course of this study, metabolome analysis played a key role in leading the direction of this research work and was also presented as a killer technology to find possible target in the production pathway that lead to the improvement of 1-butanol titer and productivity. Therefore, it successfully fulfilled the main objective of this study as laid out in Section 1.7, namely to improve 1-butanol titer and productivity in *Synechococcus elongatus* 1-butanol producing strain by identifying possible target for strain improvement in the 1-butanol biosynthesis pathway.

As general lessons obtained from this study, the iterative cycle of metabolomics-assisted strain engineering in Chapter 2 and Chapter 3 exhibited the advantage of combination of metabolomics and metabolic engineering approach. Same tactics can possibly be applied in order to find target for strain improvement in other microbial hosts. Moreover, the knowledge of the regulation of acetyl-CoA and free CoA regeneration in the CoA-dependent pathway that

are suggested in this study can be beneficial for other production pathways that related to acetyl-CoA.

Furthermore, the current state of cyanobacterial 1-butanol production system is still unable to compete with ABE fermentation and the metabolically engineered *E. coli* and *S. cerevisiae* strains economically, due to its low production titer (418.7 mg/L in 6 days). A recent report of engineered *Clostridium* species has been able to produce 19.1 g/L within 78 h [60], or 15.7 g/L using co-utilization of glucose and xylose [61]. In addition, non-native hosts such as in *Escherichia coli* (18.3 g/L in 78 hours) [21] and *Saccharomyces cerevisiae* (835 mg/L in 96 h) [62] also have higher production titer compare to cyanobacterial 1-butanol production system. However, once this cyanobacterial production system becomes industrially applicable, it holds great promise to be more economically and environmentally friendly over the ABE fermentation system. Particularly, since the system utilizes sunlight as an energy source and CO₂ as a carbon source, the substrate costs and the high carbon footprints can possibly be reduced.

In order to make cyanobacterial 1-butanol production system feasible in the future, not only does the production titer and productivity need to be improved, but the study of tolerance towards 1-butanol is also required. Despite the high productivity obtained in this study from the newly generated strain DC11, the final 1-butanol titer of this strain is still low compared to other

microbial production hosts. Several reports suggested that sensitivity of the producing strain towards 1-butanol has been known to be one of the main hurdles for improving cyanobacterial production system [13], [27]. Thus, to further improve cyanobacterial-based 1-butanol production, a comprehensive metabolome analysis to study the intrinsic effect of improved 1-butanol productivity in DC11 and the knowledge of microbial solvent responses would be highly valuable as guidance for engineering efforts aiming to increase tolerance in the future. Moreover, it has been known that the cellular response towards solvent exposures induces complex cellular response mechanisms. These include activation of general stress response genes, upregulation of heat shock proteins and efflux pumps, and alteration of membrane composition [27]. Thus, by using combination of several omics technologies, such as metabolomics, proteomics, transcriptomics, and complementing them with physiological and molecular studies, complex solvent tolerance mechanisms can be possibly revealed. This proposed strategy may be beneficial for future strain improvement of *S. elongatus* 1-butanol producing strain.

In addition to that, another potentially useful strategy for improving 1-butanol production is the optimization of the downstream process. This may involve the integration of bioprocess designs. Several *in situ* bioproduct recovery techniques have been developed to reduce the effects of product toxicity [63]. In such cases, the products are continuously removed from the

culture before it reaches its toxic concentration. These techniques are based on liquid-liquid or vapor-liquid separation mechanism. For instance, in the liquid-liquid-based techniques, culture and solvent are separated either by direct solvent addition or utilization of a membrane extraction (i.e. perstraction). On the other hand, vapor-liquid-based techniques are performed by pervaporation and gas stripping methods. Similar to perstraction, in pervaporation methods the solvents are transferred through the membrane from the culture in their gas form whereas gas stripping is operated by bubbling a nitrogen gas to the culture to extract the solvent to the gas phase [63]. By expanding *in situ* product separation techniques as well as improving the quality of membranes, further improvement of cyanobacterial-based 1-butanol production may be achieved.

Furthermore, the advantages, problems and limitations of the metabolomics strategy based on the results demonstrated in this study are as follows; the widely targeted metabolic profiling in this study was successfully found target for strain improvement. However, the metabolites coverage in this study is still limited. By expanding metabolites coverage by using other instruments, deeper metabolome analysis, such as employing flux analysis or kinetic profiling, and integration with other omics technologies will provide another insight and may further increase 1-butanol production in cyanobacterial system. Taken together, the insights obtained

from this study can be useful for future studies of engineered cyanobacteria for large scale production of 1-butanol or other important chemicals at high titers.

Acknowledgement

First of all, I would like to express my great gratitude to Fukusaki laboratory professors; Prof. Eiichiro Fukusaki, Assoc. Prof. Shuichi Shimma, Assist. Prof. Sastia Prama Putri. Their valuable and constructive suggestions helped me come up with the thesis topic and guided me over these years to achieve the final goals. During the most difficult times, they gave me the moral support and the freedom I needed to move on. Besides my supervisors, I would like to deliver my gratitude to Dr. Walter Lavina for his patient, helps and enthusiastic advice and comments on my research.

I would like to give special appreciation to Dr. James Liao for his patient guidance, encouragement and useful critiques. I also would like to thank to Derrick Chuang for his kind cooperation in cyanobacterial strain construction. I would also like to thank the rest of my thesis committee: Prof. Takeshi Omasa and Prof. Fumio Matsuda for their insightful comments which incited me to improve my doctoral dissertation from various perspectives. I would also like to thank MEXT and Japan Science and Technology (JST) through a grant awarded under the JST-NSF Strategic International Collaborative Research, SICORP for JP-US Metabolomics and National Science Foundation (NSF) MCB-1139318 for financial support throughout my study.

Dozens of people have helped and taught me immensely at Osaka University. Special thanks to my bestie Sana, for always standing by my side, helping me with English corrections

and many things related to laboratory or my doctor life. I can't thank you enough for encouraging me throughout this experience. I also wish to thank to all Fukusaki Lab members especially to my beloved friends Adinda Kadar, and Safira who were always be there whenever and wherever I need a help. Also, Adinda Wisman, Sri, Abi, Harada, Kana, Sumikura, Nakano, Nakatani, Malik, Hadi, for your supports not only in my research but also in my life here. My gratitude also goes to my friend in Indonesia: Maman Agosto, "geng pinggiran", Dinari, Naomi, and Ninda for helping me to keep my sanity this whole time through messages. To my Indonesian friends in Japan for their warm friendship, all of you are my second family here in Japan. I would to thank to Ibu Dea Indriani as well, my supervisor in ITB who recommended me to pursue a PhD in Japan. Also, to my friend Sammy Pontrelli, who helped me a lot during my study and took me to the places that I have always dreamt of, both during my stay in LA for exchange program and my graduation trip in Swiss. Finally, last but of course not least, I would like to thank my family, my father, my mother, my younger sister, Dea, for their endless love, support and encouragement in my whole life. I am thankful for all the people -I have mentioned.

"Indeed, Allah is with the patient."

(2:153)

References

- [1] S. Kim *et al.*, “PubChem 2019 update: Improved access to chemical data,” *Nucleic Acids Res.*, vol. 47, no. D1, pp. D1102–D1109, 2019.
- [2] B. Kolesinska *et al.*, “Butanol synthesis routes for biofuel production: trends and perspectives,” *Materials (Basel)*., vol. 12, no. 3, p. 350, 2019.
- [3] Y. S. Jang *et al.*, “Bio-based production of C2-C6 platform chemicals,” *Biotechnol. Bioeng.*, vol. 109, no. 10, pp. 2437–2459, 2012.
- [4] M. Kumar, Y. Goyal, A. Sarkar, and K. Gayen, “Comparative economic assessment of ABE fermentation based on cellulosic and non-cellulosic feedstocks,” *Appl. Energy*, vol. 93, pp. 193–204, 2012.
- [5] P. Dürre, “Biobutanol: An attractive biofuel,” *Biotechnol. J.*, vol. 2, no. 12, pp. 1525–1534, 2007.
- [6] M. Sauer, “Industrial production of acetone and butanol by fermentation—100 years later,” *FEMS Microbiol. Lett.*, vol. 363, no. 13, p. fnw134, 2016.
- [7] H. G. Moon, Y. S. Jang, C. Cho, J. Lee, R. Binkley, and S. Y. Lee, “One hundred years of clostridial butanol fermentation,” *FEMS Microbiol. Lett.*, vol. 363, no. 3, 2016.
- [8] D. T. Jones and D. R. Woods, “Acetone-butanol fermentation revisited,” *Microbiol. Rev.*, vol. 50, no. 4, pp. 484–524, 1986.

- [9] S. Atsumi *et al.*, “Metabolic engineering of *Escherichia coli* for 1-butanol production,” *Metab. Eng.*, vol. 10, no. 6, pp. 305–311, 2008.
- [10] Y. J. Choi, J. Lee, Y. Jang, and S. Y. Lee, “Higher Alcohols,” vol. 5, no. 5, pp. 1–10, 2014.
- [11] S. Ranganathan and C. D. Maranas, “Microbial 1-butanol production: Identification of non-native production routes and in silico engineering interventions,” *Biotechnol. J.*, vol. 5, no. 7, pp. 716–725, 2010.
- [12] C. J. Ramey, Á. Barón-Sola, H. R. Aucoin, and N. R. Boyle, “Genome engineering in cyanobacteria: Where we are and where we need to go,” *ACS Synth. Biol.*, vol. 4, no. 11, pp. 1186–1196, 2015.
- [13] Y. Wang *et al.*, “Metabolomic basis of laboratory evolution of butanol tolerance in photosynthetic *Synechocystis* sp. PCC 6803,” *Microb. Cell Fact.*, vol. 13, no. 1, pp. 1–12, 2014.
- [14] J. C. Liao, L. Mi, S. Pontrelli, and S. Luo, “Fuelling the future: Microbial engineering for the production of sustainable biofuels,” *Nat. Rev. Microbiol.*, vol. 14, no. 5, pp. 288–304, 2016.
- [15] R. E. H. Sims, W. Mabey, J. N. Saddler, and M. Taylor, “An overview of second generation biofuel technologies,” *Bioresour. Technol.*, vol. 101, no. 6, pp. 1570–1580, 2010.
- [16] M. C. Lai and E. I. Lan, “Advances in metabolic engineering of cyanobacteria for photosynthetic biochemical production,” pp. 636–658, 2015.

- [17] E. I. Lan and J. C. Liao, "Metabolic engineering of cyanobacteria for 1-butanol production from carbon dioxide," *Metab. Eng.*, vol. 13, no. 4, pp. 353–363, 2011.
- [18] E. I. Lan and J. C. Liao, "ATP drives direct photosynthetic production of 1-butanol in cyanobacteria," *Proc. Natl. Acad. Sci. U. S. A.*, vol. 109, no. 16, pp. 6018–23, 2012.
- [19] E. I. Lan, S. Y. Ro, and J. C. Liao, "Oxygen-tolerant coenzyme A-acylating aldehyde dehydrogenase facilitates efficient photosynthetic n-butanol biosynthesis in cyanobacteria," *Energy Environ. Sci.*, vol. 6, no. 9, p. 2672, 2013.
- [20] B. M. Berla, R. Saha, C. M. Immethun, C. D. Maranas, T. S. Moon, and H. B. Pakrasi, "Synthetic biology of cyanobacteria: Unique challenges and opportunities," *Front. Microbiol.*, vol. 4, no. AUG, pp. 1–14, 2013.
- [21] T. Ohtake, S. Pontrelli, W. A. Laviña, J. C. Liao, S. P. Putri, and E. Fukusaki, "Metabolomics-driven approach to solving a CoA imbalance for improved 1-butanol production in *Escherichia coli*," *Metab. Eng.*, vol. 41, no. April, pp. 135–143, 2017.
- [22] H. Nishiguchi, J. Liao, H. Shimizu, F. Matsuda, K. Uebayashi, and N. Hiasa, "Transomics data-driven, ensemble kinetic modeling for system-level understanding and engineering of the cyanobacteria central metabolism," *Metab. Eng.*, vol. 52, no. January, pp. 273–283, 2019.
- [23] M. G. Smith, S. G. Des Etages, and M. Snyder, "Microbial synergy via an ethanol-triggered pathway," *Mol. Cell. Biol.*, vol. 24, no. 9, pp. 3874–3884, 2004.

- [24] D. R. Nielsen, E. Leonard, S. H. Yoon, H. C. Tseng, C. Yuan, and K. L. J. Prather, "Engineering alternative butanol production platforms in heterologous bacteria," *Metab. Eng.*, vol. 11, no. 4–5, pp. 262–273, 2009.
- [25] B. P. Tracy, S. W. Jones, A. G. Fast, D. C. Indurthi, and E. T. Papoutsakis, "Clostridia: The importance of their exceptional substrate and metabolite diversity for biofuel and biorefinery applications," *Curr. Opin. Biotechnol.*, vol. 23, no. 3, pp. 364–381, 2012.
- [26] H. Zhu *et al.*, "Integrated OMICS guided engineering of biofuel butanol-tolerance in photosynthetic *Synechocystis* sp. PCC 6803," *Biotechnol. Biofuels*, vol. 6, no. 1, 2013.
- [27] J. Anfelt, B. Hallström, J. Nielsen, M. Uhlén, and E. P. Hudson, "Using transcriptomics to improve butanol tolerance of *Synechocystis* sp. Strain PCC 6803," *Appl. Environ. Microbiol.*, vol. 79, no. 23, pp. 7419–7427, 2013.
- [28] N. Kataoka *et al.*, "Construction of CoA-dependent 1-butanol synthetic pathway functions under aerobic conditions in *Escherichia coli*," *J. Biotechnol.*, vol. 204, pp. 25–32, 2015.
- [29] S. T. Teoh, S. Putri, Y. Mukai, T. Bamba, and E. Fukusaki, "A metabolomics-based strategy for identification of gene targets for phenotype improvement and its application to 1-butanol tolerance in *Saccharomyces cerevisiae*," *Biotechnol. Biofuels*, vol. 8, no. 1, p. 144, 2015.
- [30] E. Fukusaki and A. Kobayashi, "Plant metabolomics: potential for practical operation," *J. Biosci. Bioeng.*, vol. 100, no. 4, pp. 347–354, 2005.

- [31] S. P. Putri *et al.*, “Current metabolomics: Practical applications,” *J. Biosci. Bioeng.*, vol. 115, no. 6, pp. 579–589, 2013.
- [32] M. J. Van Der Werf, R. H. Jellema, and T. Hankemeier, “Microbial metabolomics: Replacing trial-and-error by the unbiased selection and ranking of targets,” *J. Ind. Microbiol. Biotechnol.*, vol. 32, no. 6, pp. 234–252, 2005.
- [33] Y. Dempo, E. Ohta, Y. Nakayama, T. Bamba, and E. Fukusaki, “Molar-based targeted metabolic profiling of cyanobacterial strains with potential for biological production,” *Metabolites*, vol. 4, no. 2, pp. 499–516, 2014.
- [34] H. Kato, Y. Izumi, T. Hasunuma, F. Matsuda, and A. Kondo, “Widely targeted metabolic profiling analysis of yeast central metabolites,” *J. Biosci. Bioeng.*, vol. 113, no. 5, pp. 665–673, 2012.
- [35] H. Tsugawa, M. Arita, M. Kanazawa, A. Ogiwara, T. Bamba, and E. Fukusaki, “MRMPROBS: A data assessment and metabolite identification tool for large-scale multiple reaction monitoring based widely targeted metabolomics,” *Anal. Chem.*, vol. 85, no. 10, pp. 5191–5199, 2013.
- [36] Z. Hashim, S. T. Teoh, T. Bamba, and E. Fukusaki, “Construction of a metabolome library for transcription factor-related single gene mutants of *Saccharomyces cerevisiae*,” *J. Chromatogr. B Anal. Technol. Biomed. Life Sci.*, vol. 966, pp. 83–92, 2014.

- [37] S. H. Park, S. Kim, and J. S. Hahn, "Metabolic engineering of *Saccharomyces cerevisiae* for the production of isobutanol and 3-methyl-1-butanol," *Appl. Microbiol. Biotechnol.*, vol. 98, no. 21, pp. 9139–9147, 2014.
- [38] O. V. Berezina, N. V. Zakharova, A. Brandt, S. V. Yarotsky, W. H. Schwarz, and V. V. Zverlov, "Reconstructing the clostridial n-butanol metabolic pathway in *Lactobacillus brevis*," *Appl. Microbiol. Biotechnol.*, vol. 87, no. 2, pp. 635–646, 2010.
- [39] A. M. Ruffing, "Improved free fatty acid production in cyanobacteria with *Synechococcus* sp. PCC 7002 as Host.," *Front. Bioeng. Biotechnol.*, vol. 2, no. May, p. 17, 2014.
- [40] J. W. K. Oliver, I. M. P. Machado, H. Yoneda, and S. Atsumi, "Combinatorial optimization of cyanobacterial 2,3-butanediol production," *Metab. Eng.*, vol. 22, pp. 76–82, 2014.
- [41] Y. Hirokawa, Y. Maki, and T. Hanai, "Improvement of 1,3-propanediol production using an engineered cyanobacterium, *Synechococcus elongatus* by optimization of the gene expression level of a synthetic metabolic pathway and production conditions," *Metab. Eng.*, vol. 39, no. November 2016, pp. 192–199, 2016.
- [42] S. Noguchi *et al.*, "Quantitative target analysis and kinetic profiling of acyl-CoAs reveal the rate-limiting step in cyanobacterial 1-butanol production," *Metabolomics*, vol. 12, no. 2, pp. 1–10, 2016.
- [43] H. M. Salis, E. A. Mirsky, and C. A. Voigt, "Automated design of synthetic ribosome binding

- sites to control protein expression,” *Nat. Biotechnol.*, vol. 27, no. 10, pp. 946–950, 2009.
- [44] A. Espah Borujeni, A. S. Channarasappa, and H. M. Salis, “Translation rate is controlled by coupled trade-offs between site accessibility, selective RNA unfolding and sliding at upstream standby sites,” *Nucleic Acids Res.*, vol. 42, no. 4, pp. 2646–2659, 2014.
- [45] A. M. Fathima, D. Chuang, W. A. Laviña, J. Liao, S. P. Putri, and E. Fukusaki, “Iterative cycle of widely targeted metabolic profiling for the improvement of 1-butanol titer and productivity in *Synechococcus elongatus*,” *Biotechnol. Biofuels*, vol. 11, no. 1, p. 188, Dec. 2018.
- [46] Z. Lei, D. V. Huhman, and L. W. Sumner, “Mass spectrometry strategies in metabolomics,” *J. Biol. Chem.*, vol. 286, no. 29, pp. 25435–25442, 2011.
- [47] N. E. Madala, L. A. Piater, P. A. Steenkamp, and I. A. Dubery, “Multivariate statistical models of metabolomic data reveals different metabolite distribution patterns in isonitrosoacetophenone-elicited *Nicotiana tabacum* and *Sorghum bicolor* cells,” *Springerplus*, vol. 3, no. 1, p. 254, 2014.
- [48] H. M. Salis, “The ribosome binding site calculator,” *Methods Enzymol.*, vol. 498, pp. 19–42, 2011.
- [49] Q. Hu *et al.*, “Microalgal triacylglycerols as feedstocks for biofuel production : perspectives and advances,” pp. 621–639, 2008.
- [50] S. Pontrelli *et al.*, “Author ’ s Accepted Manuscript *Escherichia coli* as a host for metabolic

- engineering,” *Metab. Eng.*, no. April, pp. 0–1, 2018.
- [51] W. Zha, S. B. Rubin-Pitel, Z. Shao, and H. Zhao, “Improving cellular malonyl-CoA level in *Escherichia coli* via metabolic engineering,” *Metab. Eng.*, vol. 11, no. 3, pp. 192–198, 2009.
- [52] P. G. Roessler, “Purification and characterization of acetyl-coa carboxylase from the diatom *Cyclotella cryptica*,” *Plant Physiol.*, vol. 92, no. 1, pp. 73–78, 1990.
- [53] K. Qiao *et al.*, “Engineering lipid overproduction in the oleaginous yeast *Yarrowia lipolytica*,” *Metab. Eng.*, vol. 29, pp. 56–65, 2015.
- [54] M. Hasslacher, A. S. Ivessa, F. Paltauf, and S. D. Kohlwein, “Acetyl-CoA carboxylase from yeast is an essential enzyme and is regulated by factors that control phospholipid metabolism,” *J. Biol. Chem.*, vol. 268, no. 15, pp. 10946–10952, 1993.
- [55] P. Xu, K. Qiao, W. S. Ahn, and G. Stephanopoulos, “Engineering *Yarrowia lipolytica* as a platform for synthesis of drop-in transportation fuels and oleochemicals,” *Proc. Natl. Acad. Sci.*, vol. 113, no. 39, pp. 10848–10853, 2016.
- [56] S. Y. Zeng *et al.*, “Recent advances in metabolic engineering of *Yarrowia lipolytica* for lipid overproduction,” *Eur. J. Lipid Sci. Technol.*, vol. 120, no. 3, pp. 1–10, 2018.
- [57] M. S. Davis, J. Solbiati, and J. E. Cronan, “Overproduction of acetyl-CoA carboxylase activity increases the rate of fatty acid biosynthesis in *Escherichia coli*,” *J. Biol. Chem.*, vol. 275, no. 37, pp. 28593–28598, 2000.

- [58] K. Kocharin, Y. Chen, V. Siewers, and J. Nielsen, "Engineering of acetyl-CoA metabolism for the improved production of polyhydroxybutyrate in *Saccharomyces cerevisiae*," *AMB Express*, vol. 2, no. 1, p. 52, 2012.
- [59] A. Taton *et al.*, "Broad-host-range vector system for synthetic biology and biotechnology in cyanobacteria," *Nucleic Acids Res.*, vol. 42, no. 17, pp. 1–16, 2014.
- [60] C. Xue, J. Zhao, C. Lu, S. T. Yang, F. Bai, and I. C. Tang, "High-titer n-butanol production by *Clostridium acetobutylicum* JB200 in fed-batch fermentation with intermittent gas stripping," *Biotechnol. Bioeng.*, vol. 109, no. 11, pp. 2746–2756, 2012.
- [61] L. Yu, M. Xu, I. C. Tang, and S. T. Yang, "Metabolic engineering of *Clostridium tyrobutyricum* for n-butanol production through co-utilization of glucose and xylose," *Biotechnol. Bioeng.*, vol. 112, no. 10, pp. 2134–2141, 2015.
- [62] S. Shi, T. Si, Z. Liu, H. Zhang, E. L. Ang, and H. Zhao, "Metabolic engineering of a synergistic pathway for n-butanol production in *Saccharomyces cerevisiae*," *Sci. Rep.*, vol. 6, no. April, p. 25675, 2016.
- [63] A. Flores, X. Wang, and D. R. Nielsen, "Recent trends in integrated bioprocesses: aiding and expanding microbial biofuel/biochemical production," *Curr. Opin. Biotechnol.*, vol. 57, pp. 82–87, 2019.

List of publication

Fathima, A. M., Chuang, D., Laviña, W. A., Liao, J., Putri, S. P., & Fukusaki, E. (2018).

Iterative cycle of widely targeted metabolic profiling for the improvement of 1-butanol titer and productivity in *Synechococcus elongatus*. *Biotechnology for Biofuels*, 11 (1).

Conference list:

Mega Fathima A, Walter Lavina, Sastia Putri, James Liao, Eiichiro Fukusaki. Application of widely targeted metabolic profiling for improvement of *Synechococcus elongatus* 1-butanol-producing strains. *68th SBJ (The Society for Biotechnology, Japan) annual meeting, Toyama, 2016* – poster presentation.

Mega Fathima A, Walter Lavina, Sastia Putri, James Liao, Eiichiro Fukusaki. Application of widely targeted metabolic profiling for improvement of *Synechococcus elongatus* 1-butanol-producing strains. *JST-NSF Metabolomics and Metabolic Engineering Workshop, Los Angeles, 2016* – oral presentation

Mega Fathima A, Walter Lavina, Sastia Putri, James Liao, Eiichiro Fukusaki. LC/MS-based widely targeted metabolomics for the improvement of 1-butanol titer in transgenic *Synechococcus elongatus*. *69th SBJ (The Society for Biotechnology, Japan) annual meeting, Tokyo, 2017* – poster presentation

Mega Fathima A, Walter Lavina, Sastia Putri, James Liao, Eiichiro Fukusaki. LC/MS-based widely targeted metabolomics for the improvement of 1- butanol titer in transgenic *Synechococcus elongatus*. *11th Metabolome symposium, Japan annual meeting, Osaka, 2017* – poster presentation

Mega Fathima A, Sastia Putri, Eiichiro Fukusaki, James Liao, Derrick Chuang. Widely targeted metabolomics-based improvement of *Synechococcus elongatus* 1-butanol-producing strain. *70th SBJ (The Society for Biotechnology, Japan) annual meeting, Osaka, 2018* – oral presentation

Mega Fathima A, Chuang Derrick, Lavina Walter Alvarez, Liao James, Putri Sastia Prama1, Fukusaki Eiichiro. Study of 1-butanol improvement in *Synechococcus elongatus*. *12th Metabolome symposium, Japan annual meeting, Tsuruoka, 2018* – poster presentation

Appendix

Figure S1

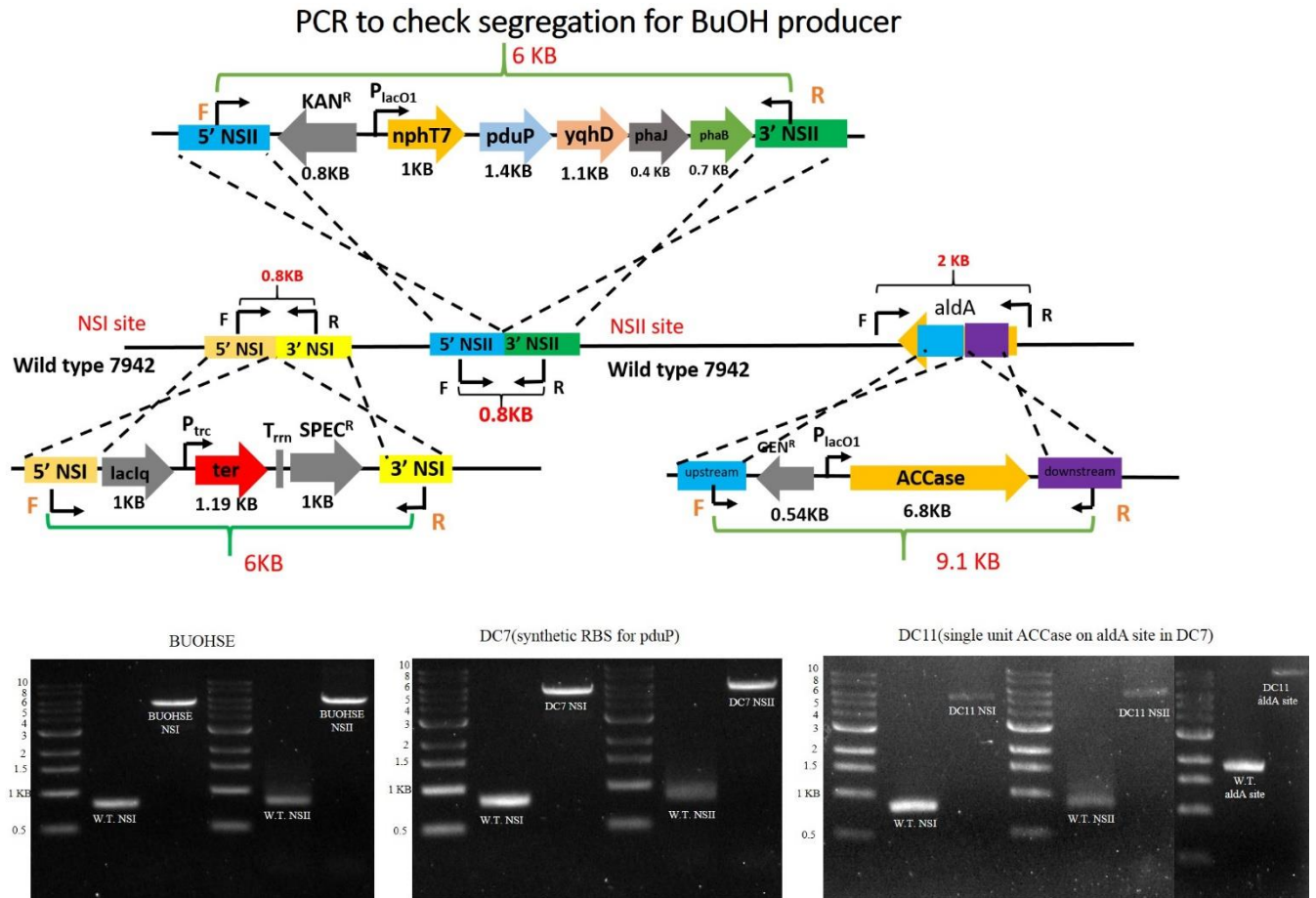


Figure S1. Colony PCR results for the segregation test in BUOHSE, DC7, and DC11 strain, W.

T. (wild type strain), NSI (neutral site I), NSII (neutral site II). *This work was done by collaborator in UCLA.*

Figure S2

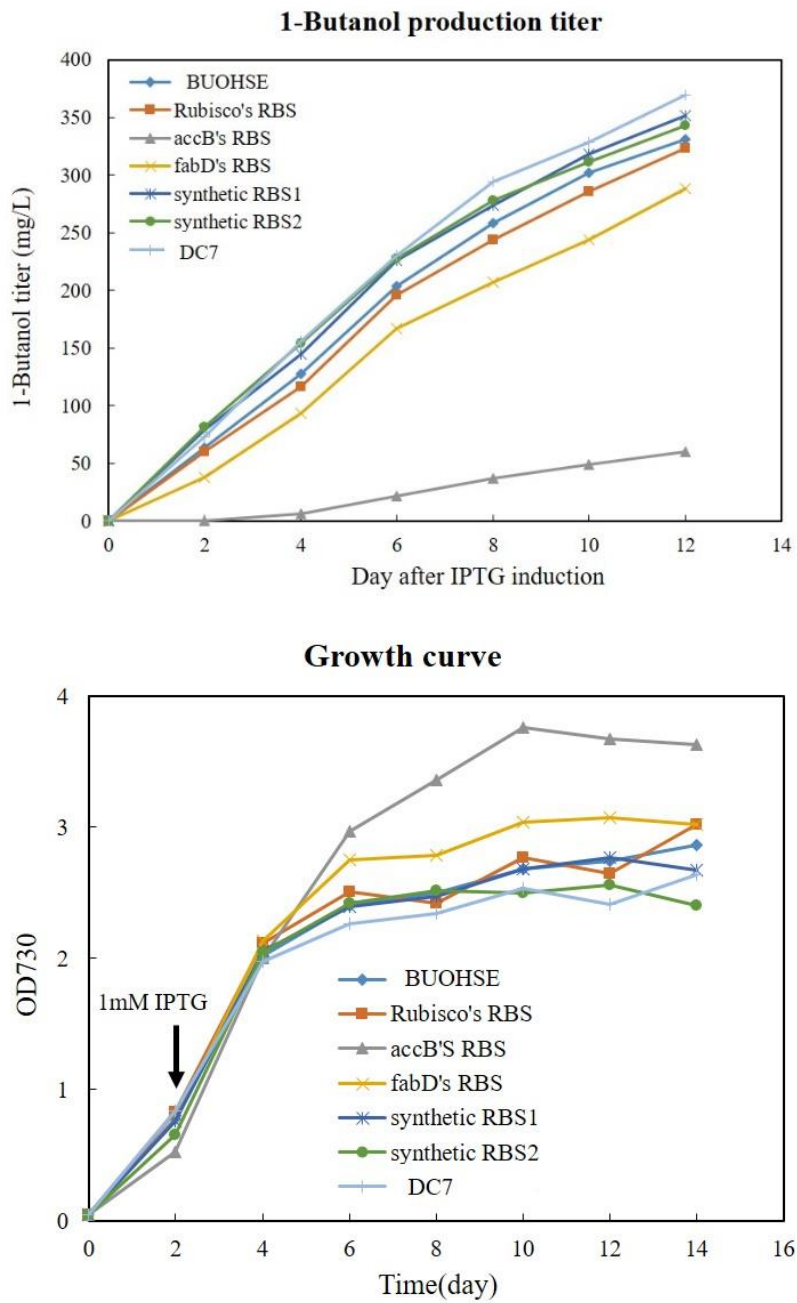


Figure S2. 1-Butanol production and cell density of *S. elongatus* obtained with the different RBS sequences.

Figure S3

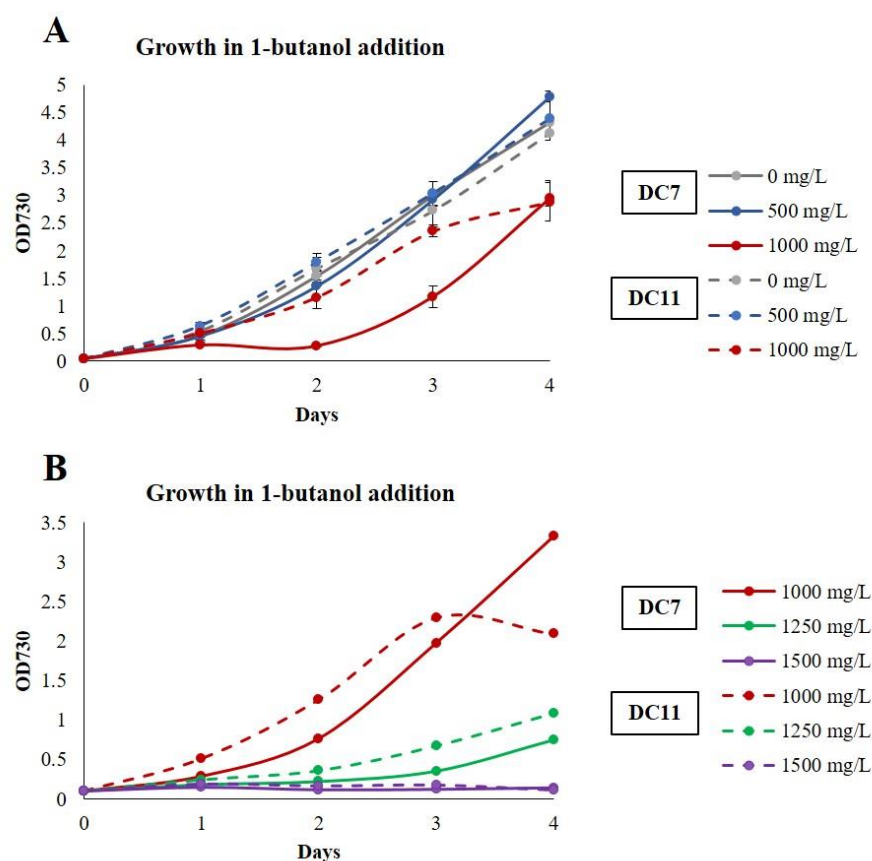


Figure S3. (A) Cell density of *S. elongatus* DC7 and DC11 at concentrations ranging from 0-1000 mg/L. (B) Cell density of *S. elongatus* DC7 and DC11 at concentrations ranging from 1000 -1500 mg/L Solid line represents DC7, while dashed line represents DC11. The error bars indicate standard deviations obtained from three replicates. The bottom graph was obtained from two replicates.

Table S1. Multiple reaction monitoring (MRM) transitions for widely targeted analysis in RP-IP-LC/QqQ-MS system

Metabolite	Precursor ion m/z	Product ion m/z	Retention Time (minute)	Target Collision Energy (V)
Arginine	173.05	131.05	1.272	15
Lysine	145.1	97.05	1.275	13
Histidine	154.05	93	1.277	21
4-Aminobutyrate	162.05	102	1.465	8
Serine	104.05	74.1	1.653	16
Asparagine	131.05	113.05	1.659	15
Glutamine	145.1	127.05	1.691	18
Threonine	118.05	74.05	1.702	16
Hydroxyproline	190.05	130.05	1.709	10
Hexose	179.05	89	1.743	19
2-Aminobutyrate	162.05	102	1.817	8
Cysteine	239.05	120.1	1.825	13
Trehalose	341.05	89.1	1.885	23
Proline	174.05	114	1.898	10

Sucrose	341.05	89.1	2.074	23
Valine	176.05	116.05	2.201	10
Cytidine	302.05	242	2.337	10
Pyridoxamine-5Phospate	247.05	230	2.453	11
Methionine	148.05	47.05	2.767	14
Guanine	150.05	133.05	3.126	21
Hypoxanthine	135.05	92	3.546	28
Tyrosine	180.05	163.05	3.554	18
Adenine	134.1	107.05	3.589	22
Isoleucine	190.05	130.05	3.638	10
Leucine	190.05	130.05	3.963	10
Xanthine	151.05	108.05	3.978	18
Glutamate	146.05	102.05	4.284	15
Uridine	243.05	110.05	4.325	17
Aspartate	132.05	88.05	4.426	14
Inosine	267.05	135.05	4.566	23
Thymine	125.05	42	4.575	18
Guanosine	282.1	150.05	4.605	21

Urate	167.1	124.05	4.699	15
Shikimate	173.05	93	4.854	17
Adenosine	266.1	134.05	4.975	25
Glycerate	105.05	75.05	5.097	13
Thymidine	301.1	241	5.151	10
Phenylalanine	164.05	147.05	5.208	18
Glycolate	75.05	47.05	5.335	13
Glyoxylate	73	73	5.754	5
G6P	259.05	97	6.303	17
Disaccharide-Phosphate	421.1	79.05	6.372	40
Mn6P	259.05	97	6.535	17
Sor6P	261.05	97	6.593	23
Pyroglutamate	188.05	128	6.618	12
Tryptophan	203.1	116.05	6.675	18
R5P	229.05	97	6.691	13
Succinic Semialdehyde	101.05	57	6.697	13
Lactate	89.05	43	6.779	14
S7P	289.1	97	6.803	21

F6P	259.05	97	6.823	17
Ara5P	229.05	97	6.982	13
G1P	259.05	79.05	7.062	28
α -Glycerophosphate	171.05	79.05	7.063	18
TPP	424.1	302.05	7.103	16
NAD	662.1	540.1	7.188	18
GAP	169.05	97	7.288	12
Orotate	155.05	111.05	7.301	14
Ru5P	229.05	97	7.459	13
CMP	322.1	79.05	7.488	28
β - Glycerophosphate	171.05	79.05	7.597	18
MEP	215.05	79.05	7.623	27
F1P	259.05	97	7.651	17
Pyruvate	87.05	43	7.782	11
R1P	229.05	79.05	7.812	25
UMP	323.1	79.05	7.951	36
AICAR	337.1	79.05	8.001	37
GMP	362.1	79.05	8.031	26

IMP	347.05	79.05	8.049	40
DHAP	169.05	97	8.085	12
TMP	321.1	195.05	8.572	20
AMP	346.1	79.05	8.618	38
Pantothenate	218.05	88	8.814	17
Nicotinate	122.05	78	8.818	16
cAMP	328.1	134.05	9.143	27
Succinate	117.05	73	9.568	15
Carbamoyl-P	140.05	79.05	9.569	22
Glutathione	306.05	143.05	9.571	20
Malate	133.05	115	9.848	17
UDP-Glu	565.05	323.05	9.878	27
XMP	363.1	211.05	9.961	20
CDP	402.1	79.05	10.021	42
Acetyl-P	139	79.05	10.045	14
2OG	145.1	101.05	10.046	10
ADP-Glu	588.05	346.05	10.069	23
Fumarate	115.05	71	10.128	10

GDP	442.1	79.05	10.131	45
6PGA	275.05	177.05	10.154	16
UDP	403.1	159	10.176	28
3PGA	185.05	97	10.181	16
Shikimate-3P	253.05	97	10.224	13
NADH	664.1	79.05	10.238	57
NADP	742.1	620.1	10.329	18
ADP	426.1	79.05	10.353	46
SBP	369.1	97	10.374	27
Citrate	191.05	87	10.399	18
FBP	339.05	97	10.423	18
PEP	167.05	79.05	10.477	15
RuBP	309.05	97	10.482	18
HMBPP	261.05	79.05	10.518	23
Isocitrate	191.05	73	10.568	22
FMN	455.1	97	10.593	27
2-Isopropylmalate	175.05	115.05	10.603	18
GTP	522.1	159	10.706	33

CTP	482.1	159	10.729	36
UTP	483.1	159	10.759	36
ATP	506.1	159	10.801	40
1,3-BPG	265.05	167.05	10.845	18
FAD	784.1	346.1	10.863	37
PRPP	389.1	177.05	10.948	21
NADPH	744.1	159.05	10.976	49
PQQ	329.1	241.05	11.051	15
D-Camphorsulfonic acid	231.1	80	11.055	32
CoA	766.1	408.1	11.105	30
3HB CoA	852.1	772.1	11.109	41
IPP,DMAPP	245.05	79.05	11.123	27
Malonyl-CoA	852.1	808.1	11.125	27
Acetyl-CoA	808.1	408.1	11.147	37
HMG-CoA	910.1	408.1	11.148	48
Crotonyl-CoA	834.1	408.1	11.299	36
Butanoyl-CoA	836.1	408.1	11.373	37

Table S2. Annotated metabolites in widely targeted analysis (74 metabolites in samples were annotated using method for 121 metabolites MRM transitions, described in Table S1).

Central metabolism	Nucleotides, nucleosides and nucleobases	Amino Acids	Others	Cofactors
R5P	Cytidine	Arginine	Butanoyl-CoA	FMN
S7P	Adenine	Histidine	Shikimate-3P	NAD
F6P	Uridine	Serine	Nicotinate	NADP
FBP	Guanosine	Asparagine	Glutathione	FAD
R5P	Thymidine	Glutamate	DHAP	PQQ
Ru5P	ADP	Threonine	Lactate	
Pyruvate	CDP	Cysteine	Pyroglutamate	
Acetyl-CoA	UDP	Proline	Disaccharide-P	
3PGA	GDP	Threonine	Glycolate	
6PGA	UTP	Valine	Hexose	
1,3-BPG	ATP	Tyrosine	Sucrose	
GAP	CTP	Aspartate		

α -Glycerophosphate	GTP	Valine
β - Glycerophosphate	AMP	Phenylalanine
Orotate	TMP	Methionine
2OG	XMP	
Acetyl-P	UMP	
Succinate	CMP	
Malate	IMP	
PEP	GMP	
RuBP	UDP-Glu	
(iso-) citrate		

Table S3. Calibration curves of acetyl-CoA, butanoyl-CoA, and free CoA, was acquired by using reversed phase- ion pairing- liquid chromatography- mass spectrometry (RP-IP-LC/QqQ-MS) system. The horizontal axis is the area ratio of monoisotopic peak to uniformly ^{13}C -labeled peak and vertical axis is naturally labeled standard amount in pmol/tube. $\text{U-}^{13}\text{C} / (\text{U-}^{13}\text{C} + \text{U-}^{12}\text{C})$ means the ratio of $\text{U-}^{13}\text{C}$ to $(\text{U-}^{13}\text{C} + \text{U-}^{12}\text{C})$ peak area in internal standard.

Metabolite	Range [pmol/tube]	Equation	R^2	$\text{U-}^{13}\text{C} / (\text{U-}^{13}\text{C} + \text{U-}^{12}\text{C})$
Acetyl-CoA	1 ~ 243	$y = 7.2294x + 6.2919$	0.992	1.00
Butanoyl-CoA	1 ~ 243	$y = 42.733x + 6.4882$	0.992	0.98
CoA	0.25 ~ 8	$y = 0.225x + 0.9567$	0.938	0.91

Table S4. Multiple reaction monitoring (MRM) transitions for absolute quantification of CoA-related metabolites by using RP-IP-LC/QqQ-MS system [42]

Metabolite	Precursor ion m/z of U- ¹² C metabolite	Precursor ion m/z of U- ¹³ C metabolite	Product ion m/z of U- ¹² C metabolite	Product ion m/z of U- ¹³ C metabolite	Target Collision Energy (V)
Acetyl-CoA	808.1	831.1	408.1	418.1	15
Butanoyl-CoA	836.1	861.1	408.1	418.1	13
CoA	766.1	79	787.1	79	21